

# The LHeC – an Experiment at the LHC



Max Klein, University of Liverpool, for the LHeC/FCC-eh Study Group



Circles in a circle  
W Kandinsky

The LHeC Project

Physics of DIS

Detector [Overview, Components]

Heavy Ion eA and AA Option

Summary

CDR: 1206.2913 J.Phys.G

Update:2007.14491, J.Phys.G  
to appear

At this workshop

Oliver Bruening: Monday HL-LHC and LHeC Option

Bruce Mellado: Higgs Physics with ep

Presented to the HK Conference, 19.1.2021.

Kevin Andre, Nestor Armesto, Oliver Bruening, Andrea Gaddi, Bernhard Holzer, John Jowett, Uta Klein, Peter Kostka, Bruce Mellado, Paul Newman, Ercan Pilicer, Alessandro Polini, Eva Villela, Yuji Yamazaki

special thanks to

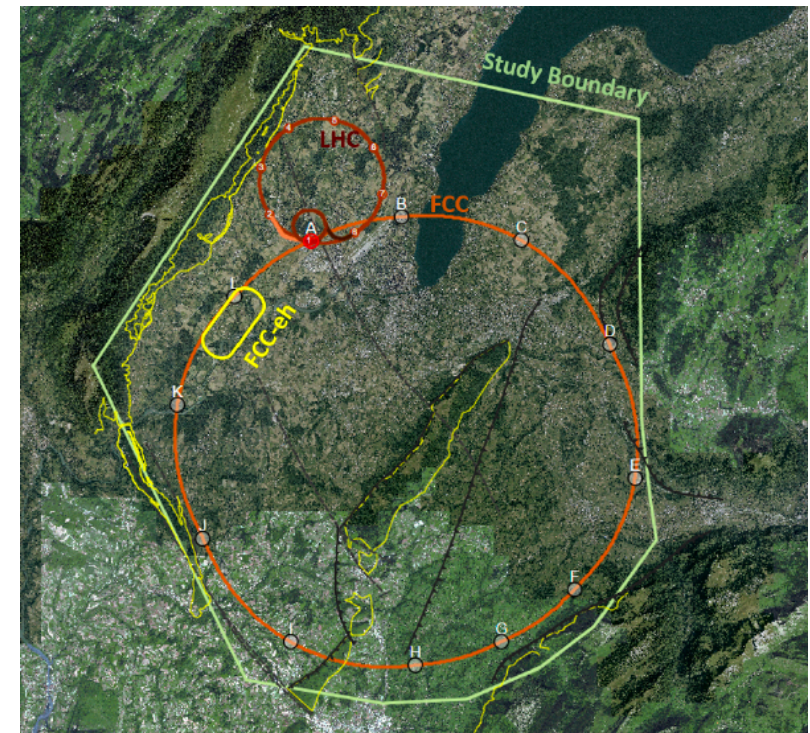
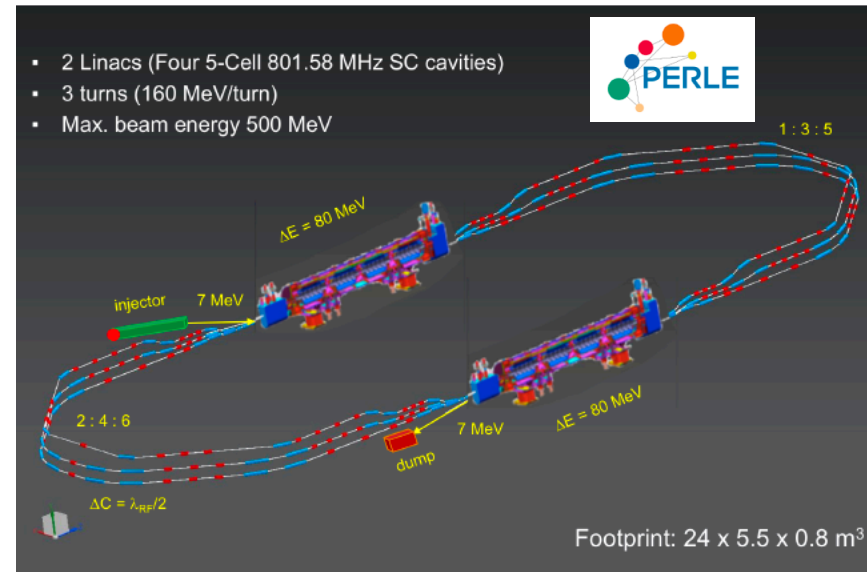
# LHeC, PERLE and FCC-eh

Powerful ERL for Experiments @ Orsay  
 CDR: 1705.08783 J.Phys.G  
 CERN-ACC-Note-2018-0086 (ESSP)

Operation: 2025+, Cost: O(20) MEuro

LHeC ERL Parameters and Configuration  
 $I_e=20\text{mA}$ , 802 MHz SRF, 3 turns  $\rightarrow$   
 $E_e=500\text{ MeV} \rightarrow$  first 10 MW ERL facility

BINP, CERN, Daresbury, Jlab, Liverpool, Orsay (IJC), +



60 x 50000 GeV<sup>2</sup>: 3.5 TeV ep collider

Operation: 2050+, Cost (of ep) O(1-2) BCHF

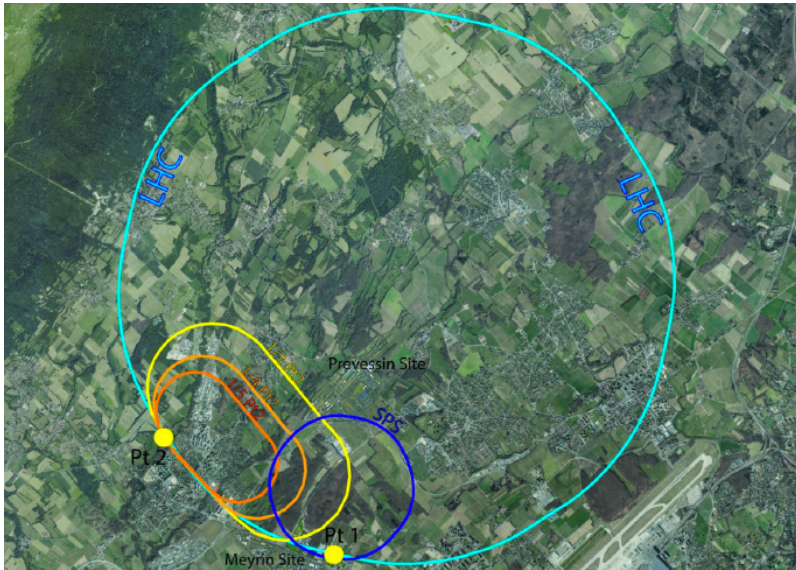
Concurrent Operation with FCC-hh

FCC CDR:

*Eur.Phys.J.ST* 228 (2019) 6, 474 Physics

*Eur.Phys.J.ST* 228 (2019) 4, 755 FCC-hh/eh

Future CERN Colliders: 1810.13022 Bordry+



50 x 7000 GeV<sup>2</sup>: 1.2 TeV ep collider

Operation: 2035+, Cost: O(1) BCHF

CDR: 1206.2913 J.Phys.G (550 citations)

Upgrade to  $10^{34}\text{ cm}^{-2}\text{s}^{-1}$ , for Higgs, BSM

CERN-ACC-Note-2018-0084 (ESSP)

arXiv:2007.14491, subm J.Phys.G

# Published in 2020

CERN-ACC-Note-2020-0002  
Geneva, July 28, 2020



## The Large Hadron-Electron Collider at the HL-LHC

LHeC and FCC-he Study Group



arXiv:2007:14491 (400 pages, 300 authors)

To be submitted to J. Phys. G

P. Agostini<sup>1</sup>, H. Aksakal<sup>2</sup>, H. Alan<sup>3</sup>, S. Alekhin<sup>4,5</sup>, P. P. Allport<sup>6</sup>, N. Andari<sup>7</sup>, K. D. J. Andre<sup>8,9</sup>, D. Angal-Kalinin<sup>10,11</sup>, S. Antusch<sup>12</sup>, L. Aperio Bella<sup>13</sup>, L. Apolinario<sup>14</sup>, R. Apsimon<sup>15,11</sup>, A. Apyan<sup>16</sup>, G. Arduini<sup>9</sup>, V. Ari<sup>17</sup>, A. Armbruster<sup>9</sup>, N. Armesto<sup>1</sup>, B. Auchmann<sup>9</sup>, K. Aulenbacher<sup>18,19</sup>, G. Azuelos<sup>20</sup>, S. Backovic<sup>21</sup>, I. Bailey<sup>15,11</sup>, S. Bailey<sup>22</sup>, F. Balli<sup>7</sup>, S. Behera<sup>23</sup>, O. Behnke<sup>24</sup>, I. Ben-Zvi<sup>25</sup>, M. Benedikt<sup>9</sup>, J. Bernauer<sup>26,27</sup>, S. Bertolucci<sup>9,28</sup>, S. S. Biswal<sup>29</sup>, J. Blümlein<sup>24</sup>, A. Bogacz<sup>30</sup>, M. Bonvini<sup>31</sup>, M. Boonekamp<sup>32</sup>, F. Bordry<sup>9</sup>, G. R. Boroun<sup>33</sup>, L. Bottura<sup>9</sup>, S. Bousson<sup>7</sup>, A. O. Bouzas<sup>34</sup>, C. Bracco<sup>9</sup>, J. Bracinik<sup>6</sup>, D. Britzger<sup>37</sup>, S. J. Brodsky<sup>36</sup>, C. Bruni<sup>7</sup>, O. Brüning<sup>9</sup>, H. Burkhardt<sup>9</sup>, O. Cakir<sup>17</sup>, R. Calaga<sup>9</sup>, A. Caldwell<sup>37</sup>, A. Cahskan<sup>38</sup>, S. Camarda<sup>9</sup>, N. C. Catalan-Lasheras<sup>9</sup>, K. Cassou<sup>39</sup>, J. Cepila<sup>40</sup>, V. Cetinkaya<sup>41</sup>, V. Chetvertkova<sup>9</sup>, B. Cole<sup>42</sup>, B. Coleppa<sup>43</sup>, A. Cooper-Sarkar<sup>22</sup>, E. Cormier<sup>44</sup>, A. S. Cornell<sup>45</sup>, R. Corsini<sup>9</sup>, E. Cruz-Alaniz<sup>8</sup>, J. Currie<sup>46</sup>, D. Curtin<sup>47</sup>, M. D'Onofrio<sup>8</sup>, J. Dainton<sup>15</sup>, E. Daly<sup>30</sup>, A. Das<sup>48</sup>, S. P. Das<sup>49</sup>, L. Dassa<sup>9</sup>, J. de Blas<sup>46</sup>, L. Delle Rose<sup>50</sup>, H. Denizli<sup>51</sup>, K. S. Deshpande<sup>52</sup>, D. Douglas<sup>30</sup>, L. Duarte<sup>53</sup>, K. Dupraz<sup>39,54</sup>, S. Dutta<sup>55</sup>, A. V. Efremov<sup>56</sup>, R. Eichhorn<sup>57</sup>, K. J. Eskola<sup>3</sup>, E. G. Ferreira<sup>1</sup>, O. Fischer<sup>58</sup>, O. Flores-Sánchez<sup>59</sup>, S. Forte<sup>60,61</sup>, A. Gaddi<sup>9</sup>, J. Gao<sup>62</sup>, T. Gehrman<sup>63</sup>, A. Gehrman-De Ridder<sup>63,64</sup>, F. Gerigk<sup>9</sup>, A. Gilbert<sup>65</sup>, F. Giuli<sup>66</sup>, A. Glazov<sup>24</sup>, N. Glover<sup>46</sup>, R. M. Godbole<sup>67</sup>, B. Goddard<sup>9</sup>, V. Gonçalves<sup>68</sup>, G. A. Gonzalez-Sprinberg<sup>53</sup>, A. Goyal<sup>69</sup>, J. Grames<sup>30</sup>, E. Granados<sup>9</sup>, A. Grassellino<sup>70</sup>, Y. O. Gunaydin<sup>2</sup>, Y. C. Guo<sup>71</sup>, V. Guzey<sup>72</sup>, C. Gwenlan<sup>22</sup>, A. Hammad<sup>12</sup>, C. C. Han<sup>73,74</sup>, L. Harland-Lang<sup>22</sup>, F. Haug<sup>9</sup>, F. Hautmann<sup>22</sup>, D. Hayden<sup>75</sup>, J. Hessler<sup>37</sup>, I. Helenius<sup>3</sup>, J. Henry<sup>30</sup>, J. Hernandez-Sanchez<sup>59</sup>, H. Hesari<sup>76</sup>, T. J. Hobbs<sup>77</sup>, N. Hod<sup>78</sup>, G. H. Hoffstaetter<sup>57</sup>, B. Holzer<sup>9</sup>, C. G. Honorato<sup>59</sup>, B. Hounsell<sup>8,11,39</sup>, N. Hu<sup>39</sup>, F. Hug<sup>18,19</sup>, A. Huss<sup>9,46</sup>, A. Hutton<sup>30</sup>, R. Islam<sup>23,79</sup>, S. Iwamoto<sup>80</sup>, S. Jana<sup>58</sup>, M. Jansova<sup>81</sup>, E. Jensen<sup>9</sup>, T. Jones<sup>8</sup>, J. M. Jowett<sup>9</sup>, W. Kaabi<sup>39</sup>, M. Kado<sup>31</sup>, D. A. Kalinin<sup>10,11</sup>, H. Karadeniz<sup>82</sup>, S. Kawaguchi<sup>83</sup>, U. Kaya<sup>84</sup>, R. A. Khalek<sup>85</sup>, H. Khanpour<sup>76,86</sup>, A. Kilic<sup>87</sup>, M. Klein<sup>8</sup>, U. Klein<sup>8</sup>, S. Kluth<sup>37</sup>, M. Köksal<sup>88</sup>, F. Kocak<sup>87</sup>, M. Korostelev<sup>22</sup>, P. Kostka<sup>8</sup>, M. Krelina<sup>89</sup>, J. Kretzschmar<sup>8</sup>, S. Kuday<sup>90</sup>, G. Kulipanov<sup>91</sup>, M. Kumar<sup>92</sup>, M. Kuze<sup>83</sup>, T. Lappi<sup>3</sup>, F. Larios<sup>34</sup>, A. Latina<sup>9</sup>, P. Laycock<sup>25</sup>, G. Lei<sup>93</sup>, E. Levitchev<sup>91</sup>, S. Levonian<sup>24</sup>, A. Levy<sup>94</sup>, R. Li<sup>95,96</sup>, X. Li<sup>62</sup>, H. Liang<sup>62</sup>, V. Litvinenko<sup>25,26</sup>, M. Liu<sup>71</sup>, T. Liu<sup>97</sup>, W. Liu<sup>98</sup>, Y. Liu<sup>99</sup>, S. Liuti<sup>100</sup>, E. Lobodzinska<sup>24</sup>, D. Longuevergne<sup>39</sup>, X. Luo<sup>101</sup>, W. Ma<sup>62</sup>, R. Machado<sup>102</sup>, S. Mandal<sup>103</sup>, H. Mäntysaari<sup>3,104</sup>, F. Marhauser<sup>30</sup>, C. Marquet<sup>105</sup>, A. Martins<sup>39</sup>, R. Martin<sup>9</sup>, S. Marzani<sup>106,107</sup>, J. McFayden<sup>9</sup>, P. McIntosh<sup>10</sup>, B. Mellado<sup>92</sup>, F. Meot<sup>57</sup>, A. Milanese<sup>9</sup>, J. G. Milhano<sup>14</sup>, B. Milityn<sup>10,11</sup>, M. Mitra<sup>108</sup>, S. Moch<sup>24</sup>, M. Mohammadi Najafabadi<sup>76</sup>, S. Mondal<sup>104</sup>, S. Moretti<sup>109</sup>, T. Morgan<sup>46</sup>, A. Morreale<sup>26</sup>, P. Nadolsky<sup>77</sup>, F. Navarra<sup>110</sup>, Z. Nergiz<sup>111</sup>, P. Newman<sup>6</sup>, J. Niehues<sup>46</sup>, E. W. Nissen<sup>9</sup>, M. Nowakowski<sup>112</sup>, N. Okada<sup>113</sup>, G. Olivier<sup>39</sup>, F. Olness<sup>77</sup>, G. Olry<sup>39</sup>, J. A. Osborne<sup>9</sup>, A. Ozansoy<sup>17</sup>, R. Pan<sup>95,96</sup>, B. Parker<sup>25</sup>, M. Patra<sup>114</sup>, H. Paukkunen<sup>3</sup>, Y. Peinaud<sup>39</sup>, D. Pellegrini<sup>9</sup>, G. Perez-Segurana<sup>15,11</sup>, D. Perini<sup>9</sup>, L. Perrot<sup>39</sup>, N. Pietralla<sup>115</sup>, E. Pilicer<sup>87</sup>, B. Pire<sup>105</sup>, J. Pires<sup>14</sup>, R. Placakyte<sup>116</sup>, M. Poelker<sup>30</sup>, R. Polifka<sup>117</sup>, A. Polini<sup>118</sup>, P. Poulou<sup>23</sup>, G. Pownall<sup>22</sup>, Y. A. Pupkov<sup>91</sup>, F. S. Queiroz<sup>119</sup>, K. Rabbertz<sup>120</sup>, V. Radescu<sup>121</sup>, R. Rahaman<sup>122</sup>, S. K. Rai<sup>108</sup>, N. Raicevic<sup>123</sup>, P. Ratoff<sup>15,11</sup>, A. Rashed<sup>124</sup>, D. Raut<sup>125</sup>, S. Raychaudhuri<sup>114</sup>, J. Repond<sup>126</sup>, A. H. Rezaeian<sup>127,128</sup>, R. Rimmer<sup>30</sup>, L. Rinolfi<sup>9</sup>, J. Rojo<sup>85</sup>, A. Rosado<sup>59</sup>, X. Ruan<sup>92</sup>, S. Russenschuck<sup>9</sup>, M. Sahin<sup>129</sup>, C. A. Salgado<sup>1</sup>, O. A. Sampayo<sup>130</sup>, K. Satendra<sup>23</sup>, N. Satyanarayan<sup>131</sup>, B. Schenke<sup>25</sup>, K. Schirm<sup>9</sup>, H. Schopper<sup>9</sup>, M. Schott<sup>19</sup>, D. Schulte<sup>9</sup>, C. Schwanenberger<sup>24</sup>, T. Sekine<sup>83</sup>, A. Senol<sup>51</sup>, A. Seryi<sup>30</sup>, S. Setiniyaz<sup>15,11</sup>, L. Shang<sup>132</sup>, X. Shen<sup>95,96</sup>, N. Shipman<sup>9</sup>, N. Sinha<sup>133</sup>, W. Slominski<sup>134</sup>, S. Smith<sup>10,11</sup>, C. Solans<sup>9</sup>, M. Song<sup>135</sup>, H. Spiesberger<sup>19</sup>, J. Stanyard<sup>9</sup>, A. Starostenko<sup>91</sup>, A. Stasto<sup>136</sup>, A. Stocchi<sup>39</sup>, M. Strikman<sup>136</sup>, M. J. Stuart<sup>9</sup>, S. Sultansoy<sup>84</sup>, H. Sun<sup>101</sup>, M. Sutton<sup>137</sup>, L. Szymanowski<sup>138</sup>, I. Tapan<sup>87</sup>, D. Tapia-Takaki<sup>139</sup>, M. Tanaka<sup>83</sup>, Y. Tang<sup>140</sup>, A. T. Tasci<sup>141</sup>, A. T. Ten-Kate<sup>9</sup>, P. Thonet<sup>9</sup>, R. Tomas-Garcia<sup>9</sup>, D. Tommasini<sup>9</sup>, D. Trbojevic<sup>25,57</sup>, M. Trott<sup>142</sup>, I. Tsurin<sup>8</sup>, A. Tudora<sup>9</sup>, I. Turk Cakir<sup>82</sup>, K. Tywoniuk<sup>143</sup>, C. Vallerand<sup>39</sup>, A. Valloni<sup>9</sup>, D. Verney<sup>39</sup>, E. Vilella<sup>8</sup>, D. Walker<sup>46</sup>, S. Wallon<sup>39</sup>, B. Wang<sup>95,96</sup>, K. Wang<sup>95,96</sup>, K. Wang<sup>144</sup>, X. Wang<sup>101</sup>, Z. S. Wang<sup>145</sup>, H. Wei<sup>146</sup>, C. Welsch<sup>8,11</sup>, G. Willering<sup>9</sup>, P. H. Williams<sup>10,11</sup>, D. Wollmann<sup>9</sup>, C. Xiaohao<sup>13</sup>, T. Xu<sup>147</sup>, C. E. Yaguna<sup>148</sup>, Y. Yamaguchi<sup>83</sup>, Y. Yamazaki<sup>149</sup>, H. Yang<sup>150</sup>, A. Yilmaz<sup>82</sup>, P. Yock<sup>151</sup>, C. X. Yue<sup>71</sup>, S. G. Zadeh<sup>152</sup>, O. Zenaiev<sup>9</sup>, C. Zhang<sup>153</sup>, J. Zhang<sup>154</sup>, R. Zhang<sup>62</sup>, Z. Zhang<sup>39</sup>, G. Zhu<sup>95,96</sup>, S. Zhu<sup>132</sup>, F. Zimmermann<sup>9</sup>, F. Zomer<sup>39</sup>, J. Zurita<sup>155,156</sup> and P. Zurita<sup>35</sup>

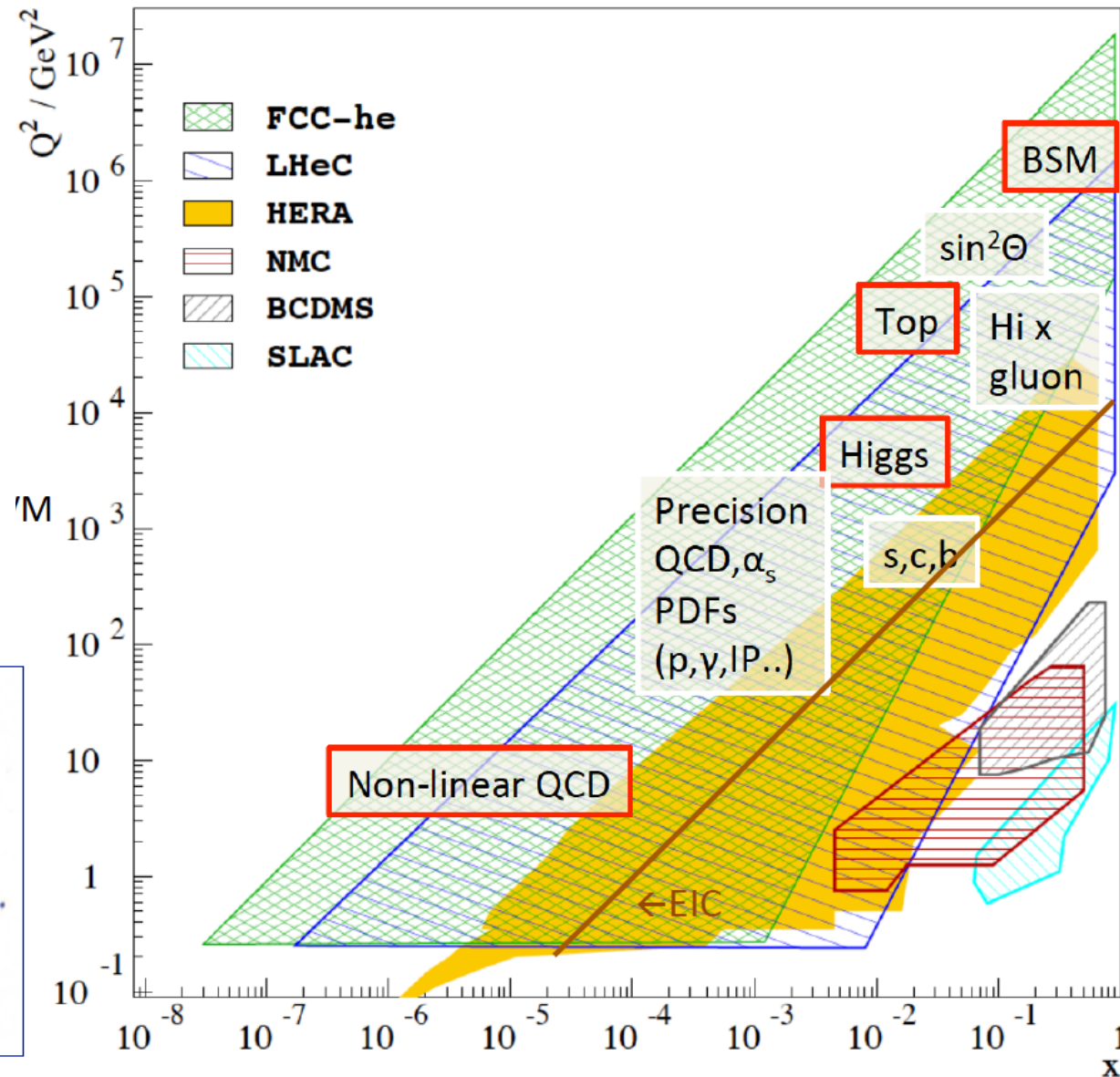
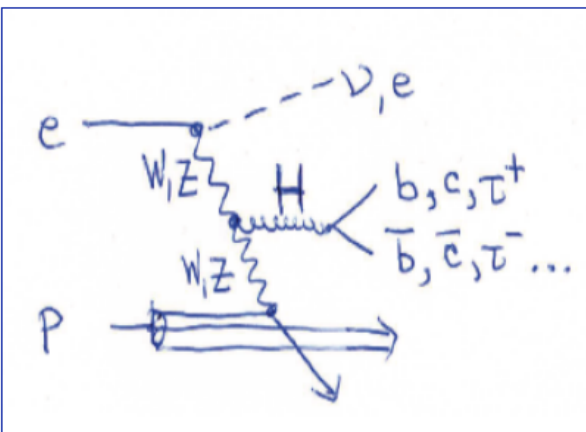
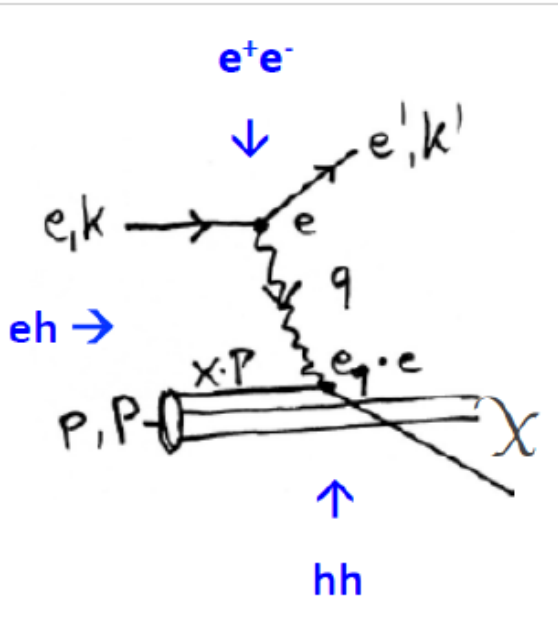
5 page summary: ECFA Newsletter Nr 5., August 20

<https://cds.cern.ch/record/2729018/files/ECFA-Newsletter-5-Summer2020.pdf>

156 Institutions involved

# Physics with Energy Frontier DIS

Deep Inelastic Scattering



**Raison(s) d'être of ep/eA at the energy frontier**

Cleanest High Resolution Microscope: QCD Discovery

Empowering the LHC/FCC Search Programme

Transformation of LHC/FCChh into high precision Higgs facility

Discovery (top, H, heavy  $\nu$ 's..) Beyond the Standard Model

A Unique Nuclear Physics Facility

# Higgs in ep and pp [LHC and FCC]

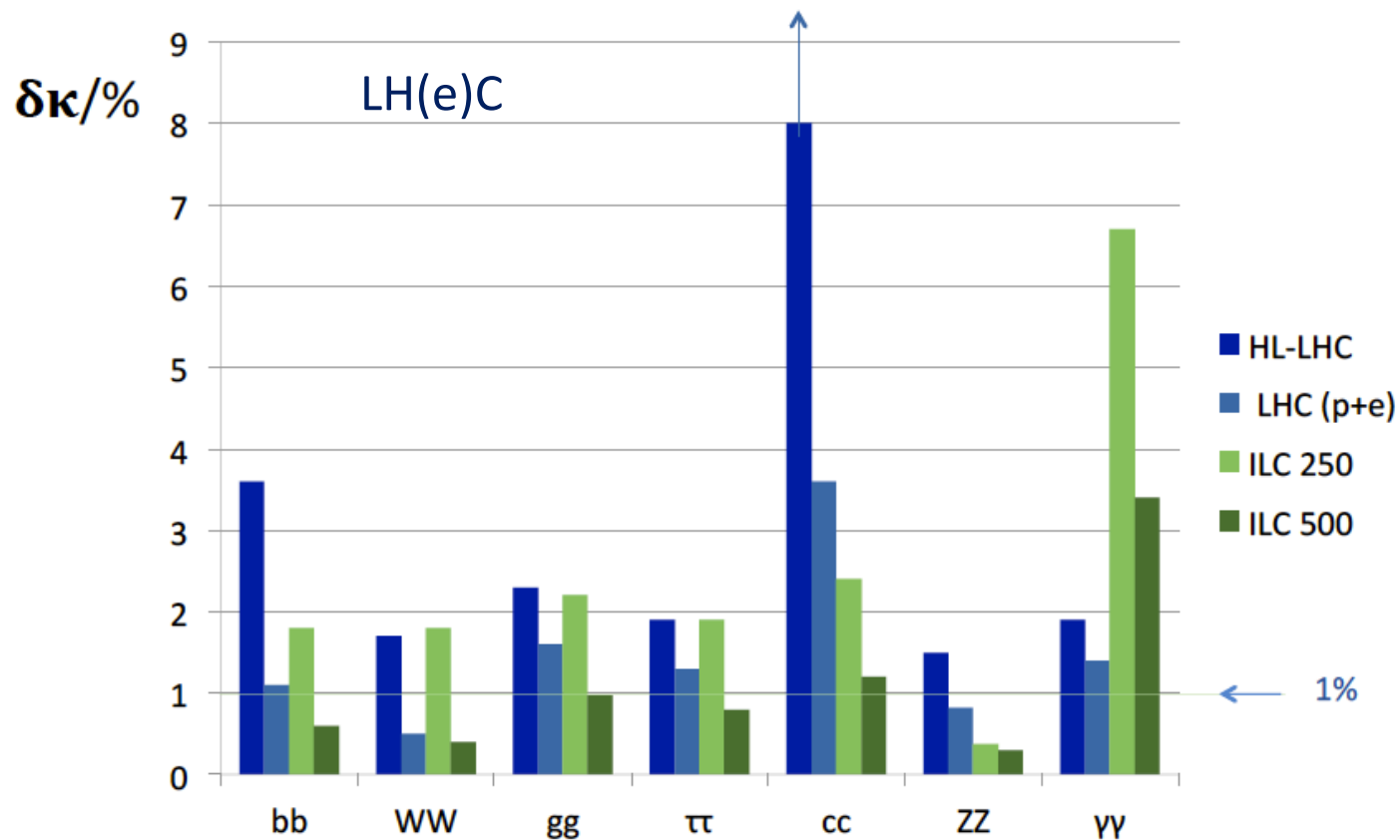


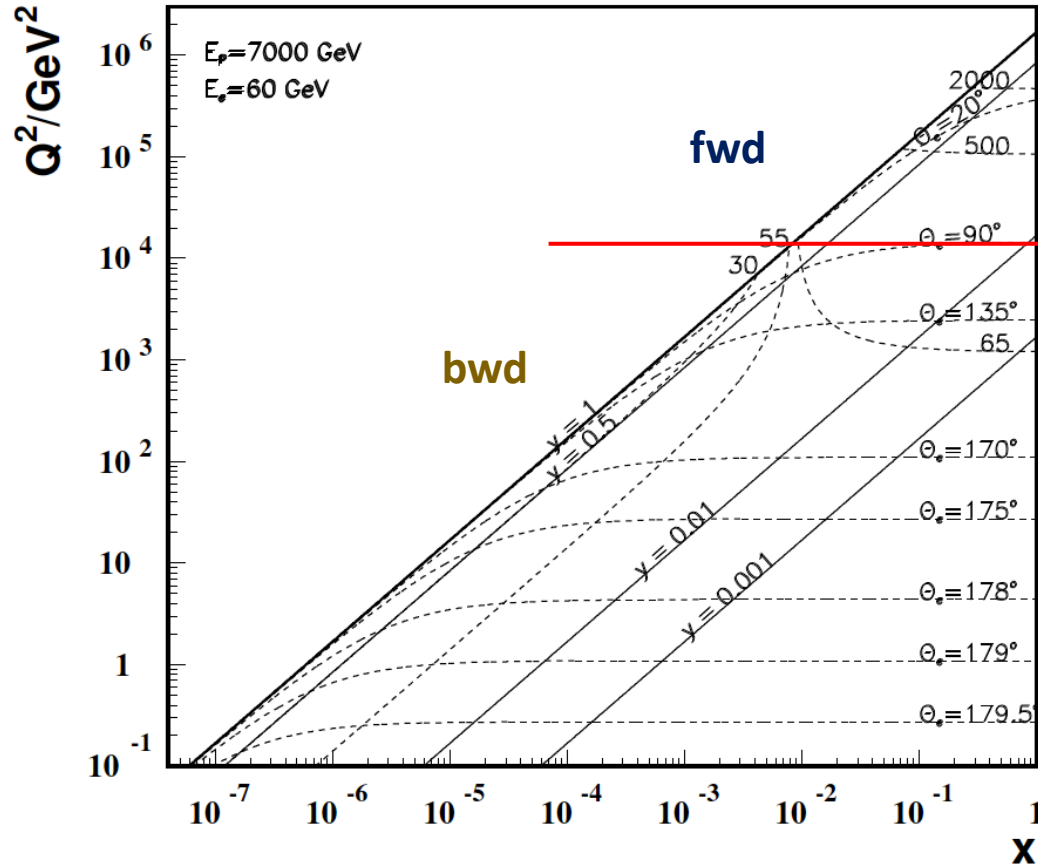
**Fig.1:** Results of prospect evaluations of the determination of Higgs couplings in the SM kappa framework for HL-LHC (dark blue), LHC with LHeC combined (p+e, light blue), ILC 250 (light green) and ILC-500 (dark green).

| Collider   | FCC-ee            | FCC-eh |
|--|-------------------|--------|
| Luminosity ( $\text{ab}^{-1}$ )                                | +1.5 @<br>365 GeV | 2      |
| Years  | 3+4               | 20     |
| $\delta\Gamma_{\text{H}}/\Gamma_{\text{H}}$ (%)                | <b>1.3</b>        | SM     |
| $\delta g_{\text{HZZ}}/g_{\text{HZZ}}$ (%)                     | <b>0.17</b>       | 0.43   |
| $\delta g_{\text{HWW}}/g_{\text{HWW}}$ (%)                     | <b>0.43</b>       | 0.26   |
| $\delta g_{\text{Hbb}}/g_{\text{Hbb}}$ (%)                     | <b>0.61</b>       | 0.74   |
| $\delta g_{\text{Hcc}}/g_{\text{Hcc}}$ (%)                     | <b>1.21</b>       | 1.35   |
| $\delta g_{\text{Hgg}}/g_{\text{Hgg}}$ (%)                     | <b>1.01</b>       | 1.17   |
| $\delta g_{\text{H}\tau\tau}/g_{\text{H}\tau\tau}$ (%)         | <b>0.74</b>       | 1.10   |
| $\delta g_{\text{H}\mu\mu}/g_{\text{H}\mu\mu}$ (%)             | <b>9.0</b>        | n.a.   |
| $\delta g_{\text{H}\gamma\gamma}/g_{\text{H}\gamma\gamma}$ (%) | <b>3.9</b>        | 2.3    |
| $\delta g_{\text{H}tt}/g_{\text{H}tt}$ (%)                     | –                 | 1.7    |
| $\text{BR}_{\text{EXO}}$ (%)                                   | <b>&lt; 1.0</b>   | n.a.   |

Prospects for high precision measurements of **Higgs couplings at FCC ee and ep**. Note ee gets the width with Z recoil. ee is mainly ZHZ, while ep is mainly WWH: complementary also to pp

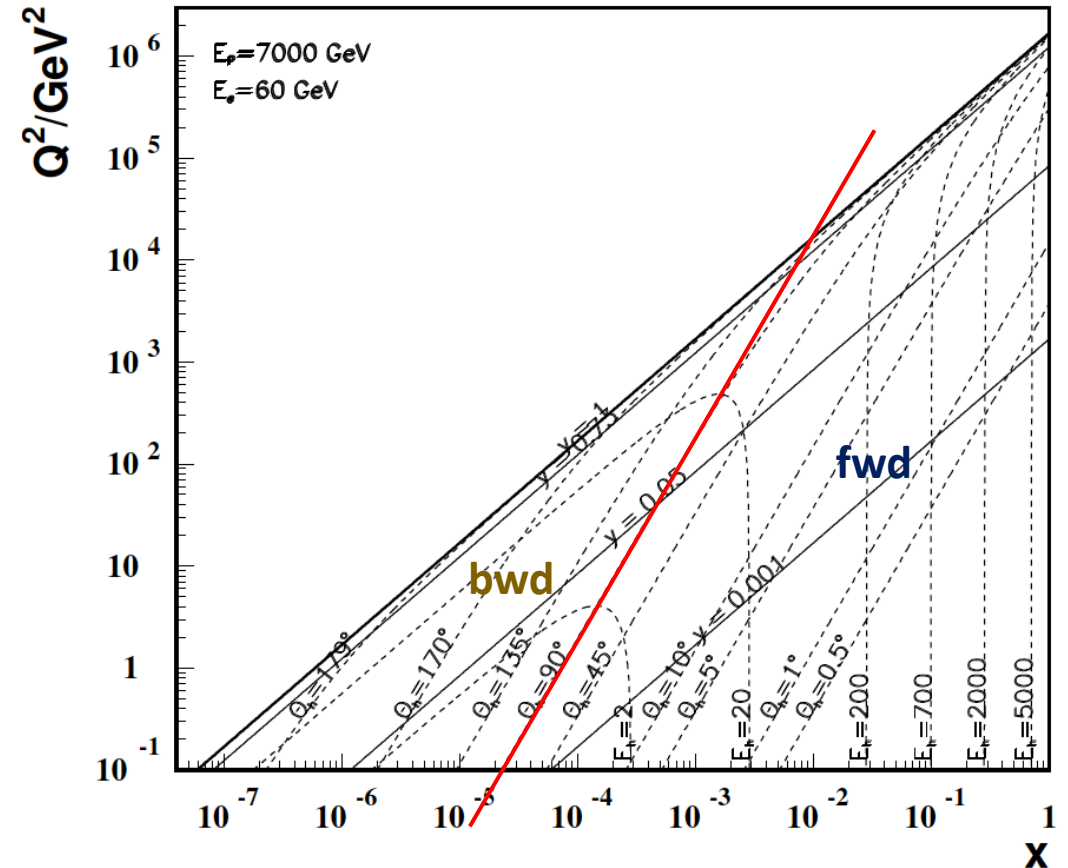
# Kinematics: fwd: in p beam direction, bwd: e direction

LHeC - electron kinematics



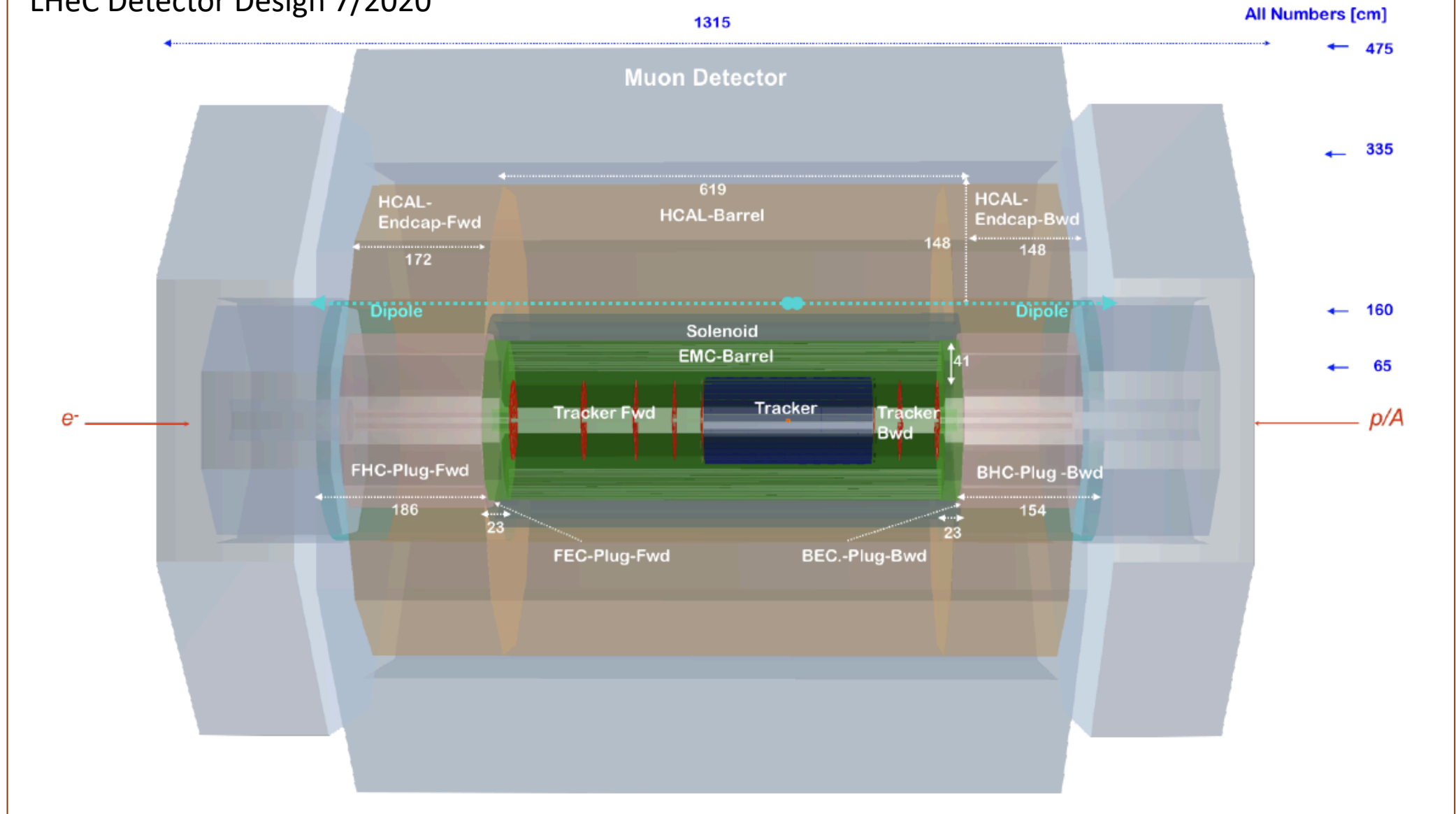
**Electrons** in bwd direction have low energy ( $E'_e < E_e$  beam)  
 in fwd direction high energy up to  $E_p$ , Rutherford backscattering  
 $Q^2=1 \text{ GeV}^2$  is  $179^\circ$ , or  $\eta = 4.74 = \ln \tan \theta/2$ ,  $\sim E_e^2$  !

LHeC - hadronic final state kinematics



Hadrons in bwd direction have low energy  $E_h < E_e$  beam  
 in fwd direction hadrons carry energy up to  $E_p$  beam

→ Asymmetric energy coverage of LHeC detector. Fwd region: resembles hh conditions



No pile up, low radiation wrt pp; high precision through overconstrained kinematics: e-h; modular for rapid installation  
 Tracker radius 40 → 60cm, B 3.5T; LxD = 13 x 9m<sup>2</sup> [CMS 21 x 15m<sup>2</sup>, ATLAS 45 x 25 m<sup>2</sup>].

|   |            |   |            |
|---|------------|---|------------|
| <b>11 Detector Requirements</b>                                 | <b>482</b> | <b>13 Forward and Backward Detectors</b>            | <b>561</b> |
| 11.1 Cost and magnets   | 483        | 13.1 Luminosity measurement and electron tagging    | 561        |
| 11.2 Detector acceptance  | 484        | 13.1.1 Options                                      | 562        |
| 11.2.1 Kinematic reconstruction                                 | 484        | 13.1.2 Use of the main LHeC detector                | 562        |
| 11.2.2 Acceptance for the scattered electron                    | 485        | 13.1.3 Dedicated luminosity detectors in the tunnel | 563        |
| 11.2.3 Acceptance for the hadronic final state                  | 487        | 13.1.4 Small angle electron tagger                  | 564        |
| 11.2.4 Acceptance at the High Energy LHC                        | 489        | 13.1.5 Summary and open questions                   | 566        |
| 11.2.5 Energy resolution and calibration                        | 491        | 13.2 Polarimeter                                    | 567        |
| 11.2.6 Tracking requirements                                    | 492        | 13.2.1 Polarisation from the scattered photons      | 568        |
| 11.2.7 Particle identification requirements                     | 495        | 13.2.2 Polarisation from the scattered electrons    | 569        |
| 11.3 Summary of the requirements on the LHeC detector           | 495        | 13.3 Zero degree calorimeter                        | 569        |
| <b>12 Central Detector</b>                                      | <b>497</b> | 13.3.1 ZDC detector design                          | 569        |
| 12.1 Basic detector description                                 | 497        | 13.3.2 Neutron calorimeter                          | 569        |
| 12.1.1 Baseline detector layout                                 | 503        | 13.3.3 Proton calorimeter                           | 570        |
| 12.1.2 An alternative solenoid placement - option B             | 505        | 13.3.4 Calibration and monitoring                   | 571        |
| 12.2 Magnet design  | 507        | 13.4 Forward proton detection                       | 571        |
| 12.2.1 Magnets configuration                                    | 507        | <b>14 Detector Assembly and Integration</b>         | <b>577</b> |
| 12.2.2 Detector solenoid  | 507        | 14.1 Detector assembly on surface                   | 578        |
| 12.2.3 Detector integrated e-beam bending dipoles               | 511        | 14.2 Detector lowering and integration underground  | 578        |
| 12.2.4 Cryogenics for magnets and calorimeter                   | 512        | 14.3 Maintenance and opening scenario               | 579        |
| 12.3 Tracking detector  | 514        | 14.4 Timelines                                      | 579        |
| 12.3.1 Tracking Detector - Baseline Layout                      | 515        |   |            |
| 12.3.2 Performance  | 516        |   |            |
| 12.3.3 Tracking detector design criteria and possible solutions | 519        |   |            |
| 12.4 Calorimetry  | 524        |   |            |
| 12.4.1 The barrel electromagnetic calorimeter                   | 525        |   |            |
| 12.4.2 The hadronic barrel calorimeter                          | 526        |   |            |
| 12.4.3 Endcap calorimeters                                      | 529        |   |            |
| 12.5 Calorimeter simulation                                     | 529        |   |            |
| 12.5.1 The barrel LAr calorimeter simulation                    | 530        |   |            |
| 12.5.2 The barrel tile calorimeter simulation                   | 531        |   |            |
| 12.5.3 Combined liquid argon and tile calorimeter simulation    | 533        |   |            |
| 12.5.4 Lead-Scintillator electromagnetic option                 | 533        |   |            |
| 12.5.5 Forward and backward inserts calorimeter simulation      | 537        |   |            |
| 12.6 Calorimeter summary  | 545        |   |            |
| 12.7 Muon detector  | 546        |   |            |
| 12.7.1 Muon detector design                                     | 547        |   |            |
| 12.7.2 The LHeC muon detector options                           | 549        |   |            |
| 12.7.3 Forward muon extensions                                  | 550        |   |            |
| 12.7.4 Muon detector summary                                    | 551        |   |            |
| 12.8 Event and detector simulations                             | 553        |   |            |
| 12.8.1 Pythia6  | 553        |   |            |
| 12.8.2 1 MeV neutron equivalent                                 | 554        |   |            |
| 12.8.3 Nearest neighbour  | 555        |   |            |
| 12.8.4 Cross checking   | 558        |   |            |
| 12.8.5 Future goals   | 560        |   |            |

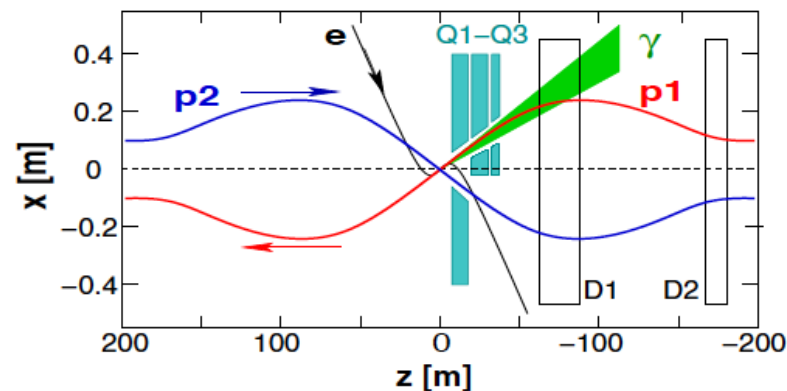
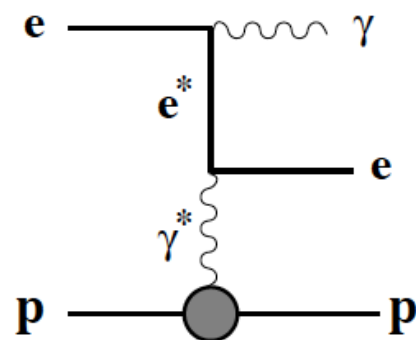


**LHeC Detector in the CDR (1206.2913)**



# Bethe Heitler - Luminosity measurement at the LHeC

CDR  
1206.2913  
JPhysG39  
075001(12)  
p561-566



| Method          | Stat. error | Syst.error | Systematic error components  | Application                     |  |
|-----------------|-------------|------------|--|---------------------------------|--|
| BH ( $\gamma$ ) | 0.05%/sec   | 1–5%       | $\sigma(E \gtrsim 10\text{GeV})$<br>acceptance, $A$<br>$E$ -scale, pileup  | 0.5%<br>$10\%(1-A)$<br>0.5 – 4% | Monitoring, tuning,<br>short term variations     |
| BH ( $e$ )      | 0.2%/sec    | 3–6%       | $\sigma(E \gtrsim 10\text{GeV})$<br>acceptance<br>background<br>$E$ -scale | 0.5%<br>2.5 – 5%<br>1%<br>1%    | Monitoring, tuning,<br>short term variations     |
| QEDC            | 0.5%/week   | 1.5%       | $\sigma(\text{el/inel})$<br>acceptance<br>vertex eff.<br>$E$ -scale        | 1%<br>1%<br>0.5%<br>0.3%        | Absolute $\mathcal{L}$ ,<br>global normalisation |
| NC DIS          | 0.5%/h      | 2.5%       | $\sigma(y < 0.6)$<br>acceptance<br>vertex eff.<br>$E$ -scale               | 2%<br>1%<br>1%<br>0.3%          | Relative $\mathcal{L}$ ,<br>mid-term variations  |

LR: photon detector  
← acceptance 95%

→ Luminosity from  
BH photons to 1%

BH to another order

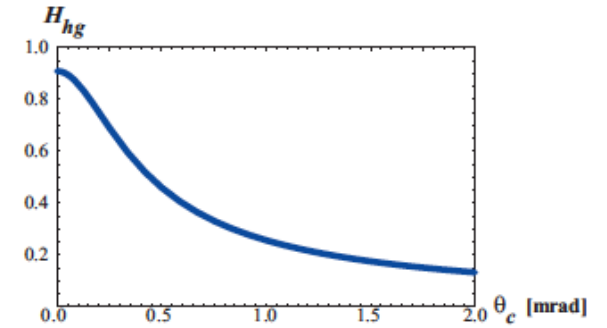
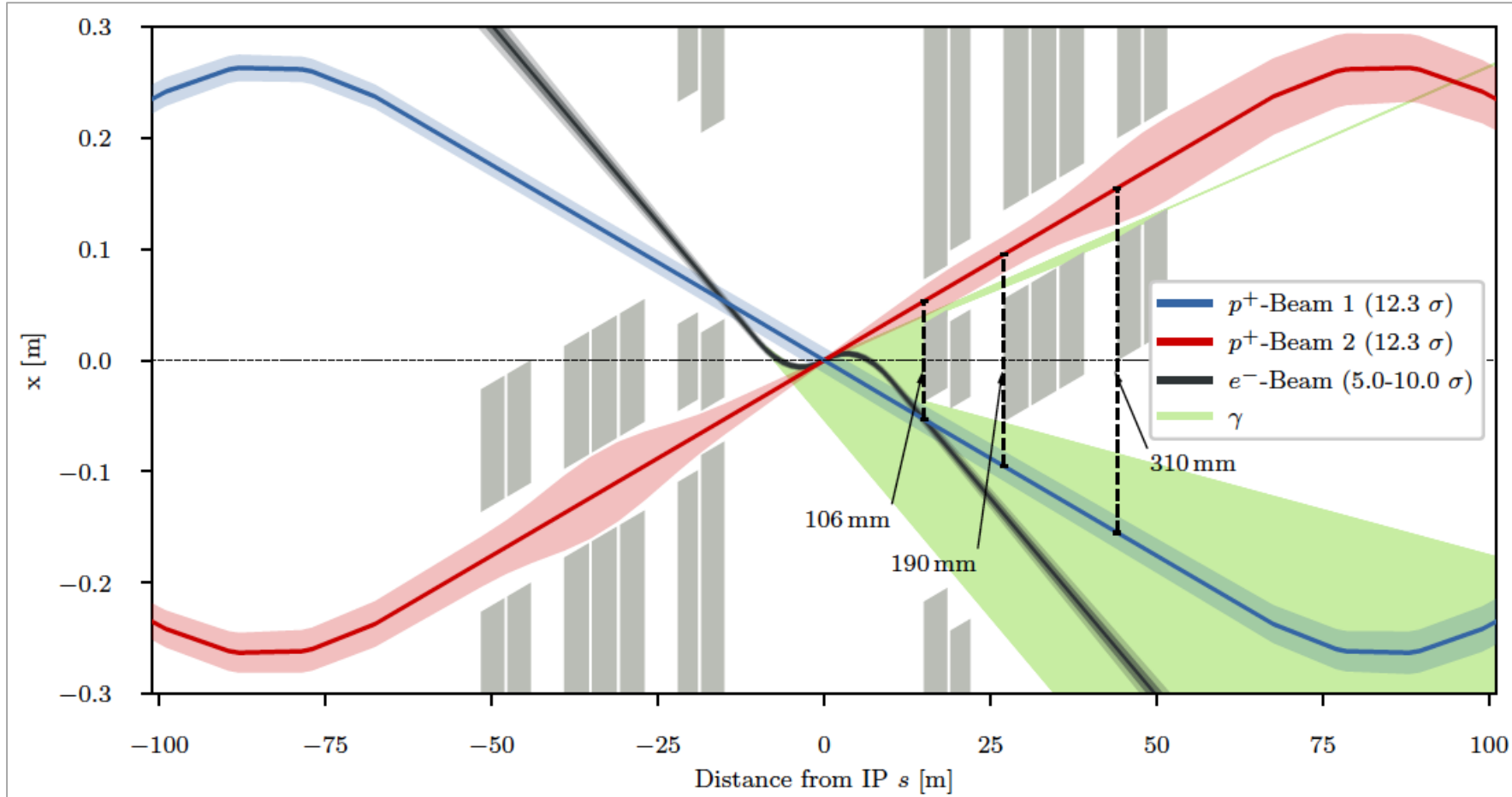
... BH( $e$ ), QEDC,  $F_2$   
as cross checks

Forward  
Taggers:

See Yuji  
Yamazaki  
at ICHEP  
and in  
2007.14491

Table 13.1: Dominant systematics for various methods of luminosity measurement.

# 3-beam ep/eA Interaction Region



$$H_{hg} = \frac{\sqrt{\pi} z e^{z^2} \operatorname{erfc}(z)}{S},$$

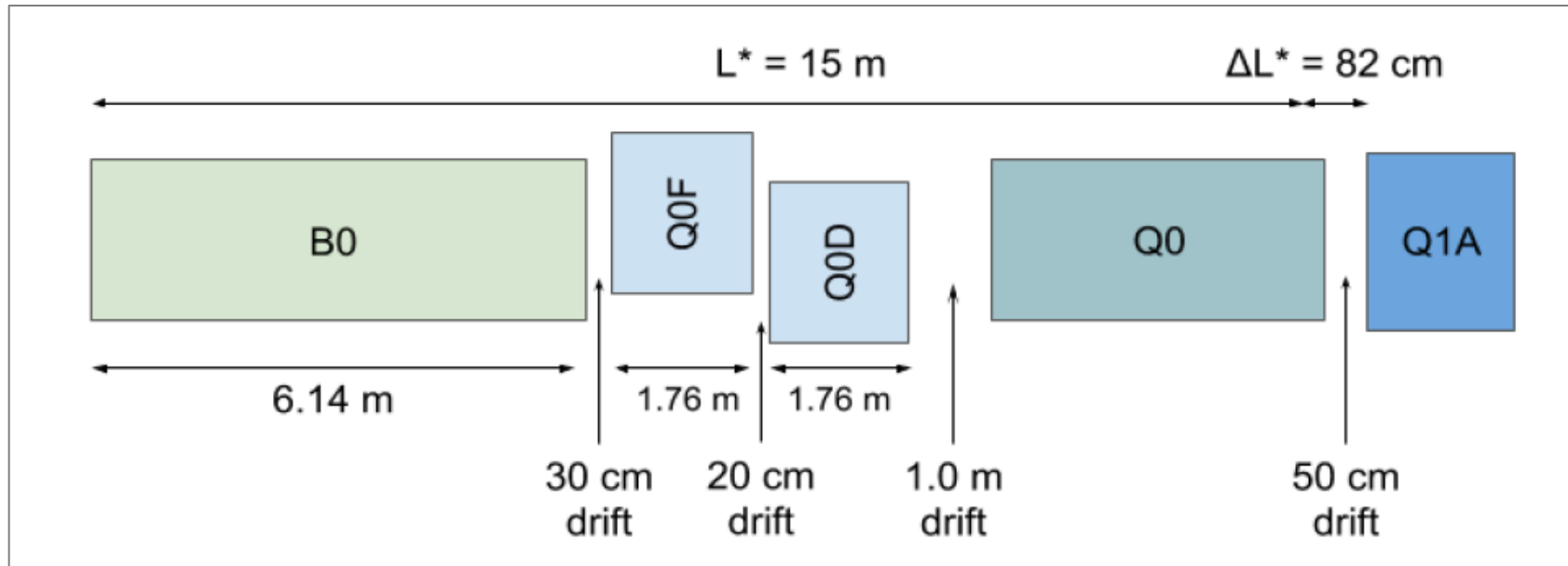
$$z \equiv 2 \frac{(\beta_e^* / \sigma_{z,p})(\epsilon_e / \epsilon_p)}{\sqrt{1 + (\epsilon_e / \epsilon_p)^2}} S$$

$$S \equiv \sqrt{1 + \frac{\sigma_{x,p}^2 \theta_c^2}{8 \sigma_p^{*2}}}$$

Synchronous ep/pp operation! Non-interacting p beam to freely pass: aperture  
 Matching e and p beam sizes (experience from HERA, also for magnet placement)

Head-on collisions  $\rightarrow$   
 Dipole magnet before  
 Hadron Calorimeter

# LHeC IR modified for dual purpose



Optimisation of synchrotron radiation (power and  $E_{\text{crit}}$ )

|                   |     | LHeC | HERA |
|-------------------|-----|------|------|
| $E_{\text{crit}}$ | keV | 270  | 150  |
| Synrad            |     |      |      |
| Power             | kW  | 30   | 28   |

Detector dipole

Staggered quads

Half-quad (NC)

First of triplet quadrupoles

For ep/A: synchronous with pp/AA in GPDs and LHCb – keep non-colliding beam apart with option of pp/AA the non-colliding beam needs to be kept inside pipe: then: shift transversely (as in regular injection mode) and possibly in time  
 For pp/AA in IP2: no electron beam in. Collisions at nominal IP (or shifted by 25/4ns)

It will look like.....a stretched and squeezed ATLAS solenoid,  
 2 T scaled up to 3.5T (2 layer coil, slightly less free bore but a bit longer)



Relatively small bore but long, and efficient coil with 1.8 m free bore, 7.1 m long

- $\approx 11$  km Al stabilized NbTi/Cu superconductor for 10 kA
- $\approx 80$  MJ stored energy and  $\approx 24$  t mass including cryostat.

H ten Kate (EP-RD, 16.3.18)

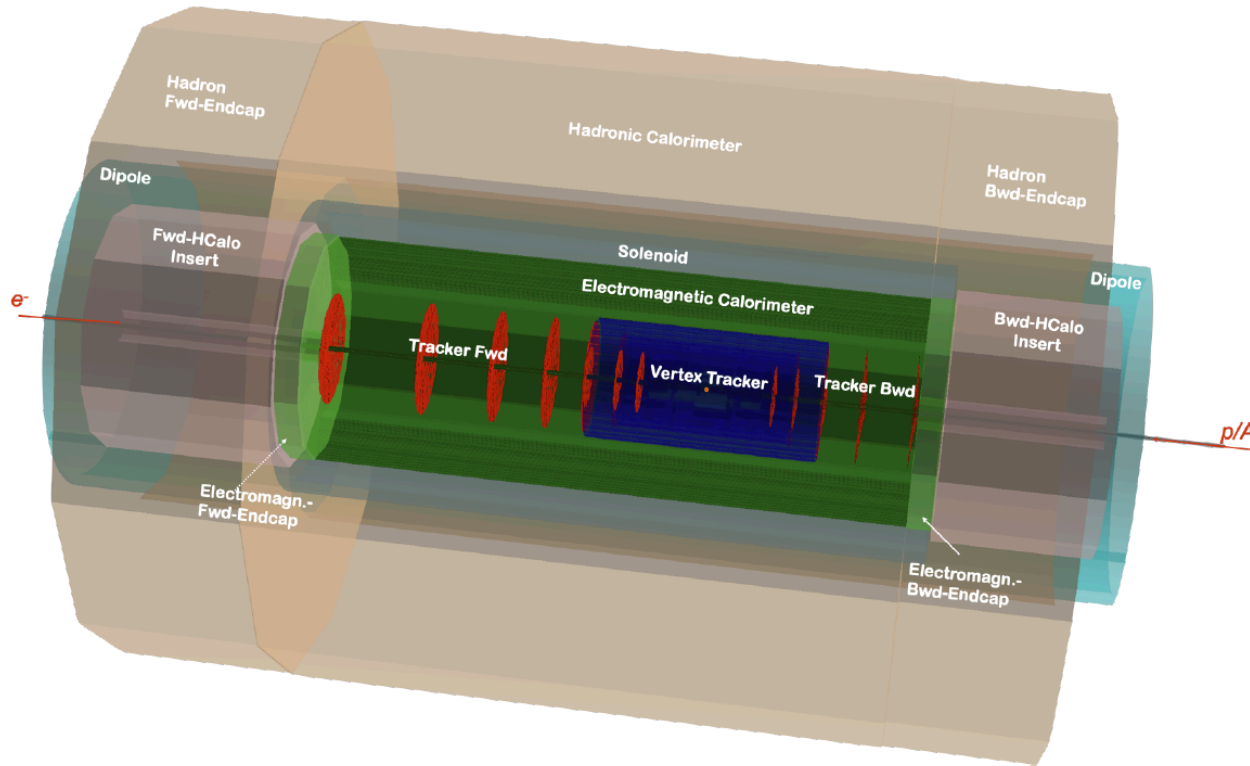
**No specific R&D needed, except detailed analysis of the dipole load case**

- Design concept: minimum cost, R&D and risk, relies on present technology for detectors magnets
- **3.5 T Solenoid & 2 Dipoles** in same cryostat around EMC, Muon tagging chambers in outer layer
- **Solenoid and dipoles have a common support cylinder in a single cryostat**; free bore of 1.8 m; extending along the detector with a length of 10 m.

For magnet specs, see  
 CDR: arXiv:1206.2913

New ideas on  
 thin magnets  
 cf. E Perez at  
 FCC workshop

# LHeC Calorimeters



Complete coverage to  $\pm 5$  in (pseudo)rapidity

Central Region: 2012: LAr, 2020 Sci/Fe option.

Forward Region: dense, high energy jets of few TeV

H  $\rightarrow$  bb and other reactions demand resolution of HFS

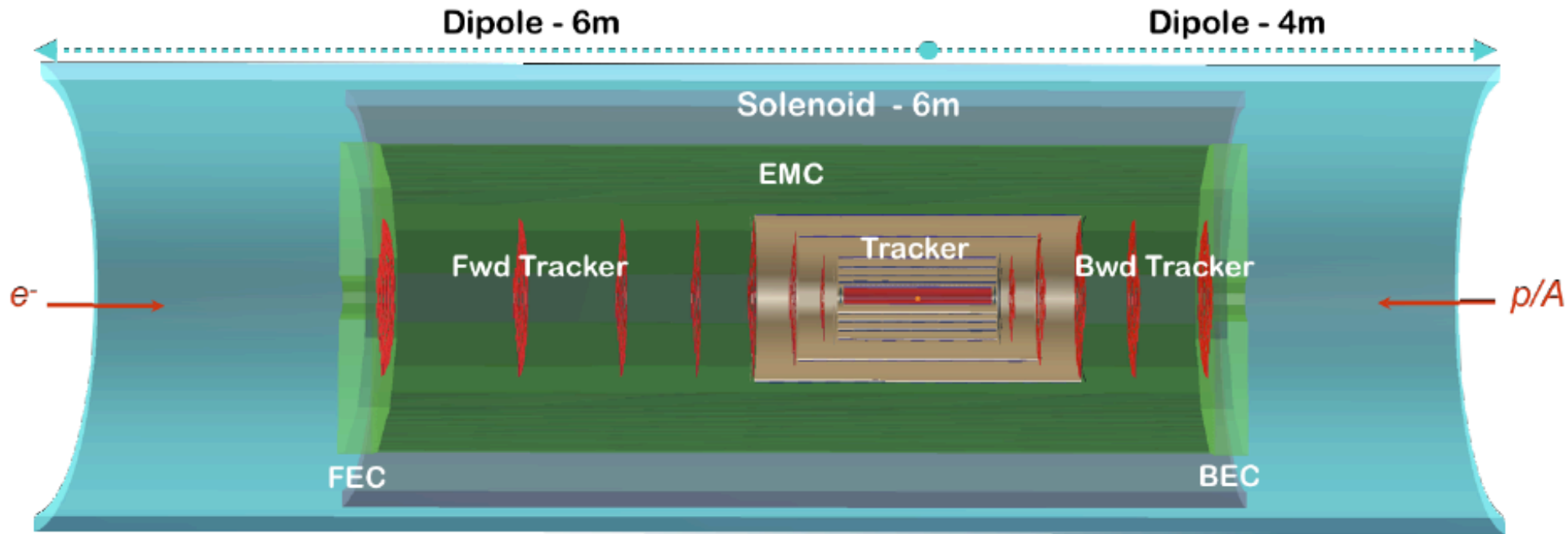
Backward Region: in DIS only deposits of  $E < E_e$

## Barrel Calorimeters

## Forward/Backward Calorimeters

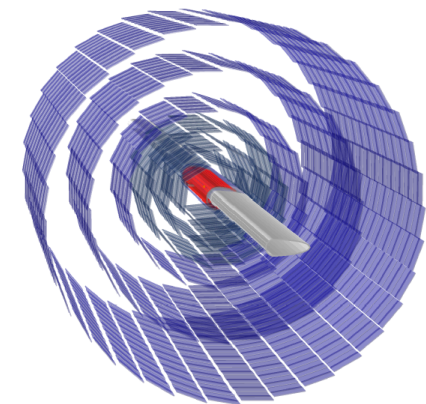
| Calo (LHeC)                            | EMC          |                   | HCAL              |                   |
|--|--------------|-------------------|-------------------|-------------------|
|  | Barrel       | Ecap Fwd          | Barrel            | Ecap Bwd          |
| Readout, Absorber Layers               | Sci,Pb<br>38 | Sci,Fe<br>58      | Sci,Fe<br>45      | Sci,Fe<br>50      |
| Integral Absorber Thickness [cm]       | 16.7         | 134.0             | 119.0             | 115.5             |
| $\eta_{\max}, \eta_{\min}$             | 2.4, -1.9    | 1.9, 1.0          | 1.6, -1.1         | -1.5, -0.6        |
| $\sigma_E/E = a/\sqrt{E} \oplus b$ [%] | 12.4/1.9     | 46.5/3.8          | 48.23/5.6         | 51.7/4.3          |
| $\Lambda_I / X_0$                      | $X_0 = 30.2$ | $\Lambda_I = 8.2$ | $\Lambda_I = 8.3$ | $\Lambda_I = 7.1$ |
| Total area Sci [m <sup>2</sup> ]       | 1174         | 1403              | 3853              | 1209              |

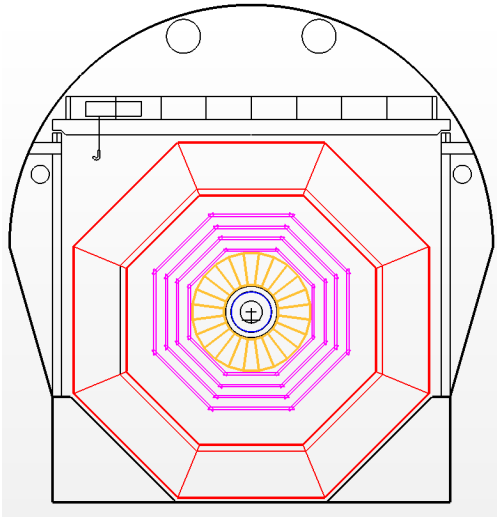
| Calo (LHeC)                            | FHC               | FEC          | BEC          | BHC               |
|--|-------------------|--------------|--------------|-------------------|
|  | Plug Fwd          | Plug Fwd     | Plug Bwd     | Plug Bwd          |
| Readout, Absorber Layers               | Si,W<br>300       | Si,W<br>49   | Si,Pb<br>49  | Si,Cu<br>165      |
| Integral Absorber Thickness [cm]       | 156.0             | 17.0         | 17.1         | 137.5             |
| $\eta_{\max}, \eta_{\min}$             | 5.5, 1.9          | 5.1, 2.0     | -1.4, -4.5   | -1.4, -5.0        |
| $\sigma_E/E = a/\sqrt{E} \oplus b$ [%] | 51.8/5.4          | 17.8/1.4     | 14.4/2.8     | 49.5/7.9          |
| $\Lambda_I / X_0$                      | $\Lambda_I = 9.6$ | $X_0 = 48.8$ | $X_0 = 30.9$ | $\Lambda_I = 9.2$ |
| Total area Si [m <sup>2</sup> ]        | 1354              | 187          | 187          | 745               |



Inner Tracker  
 Rapidity to  $\sim 5$   
 $r_0 = 60$  cm  
 impact resolution  
 5-10  $\mu\text{m}$   
 40.7  $\text{m}^2$  Si

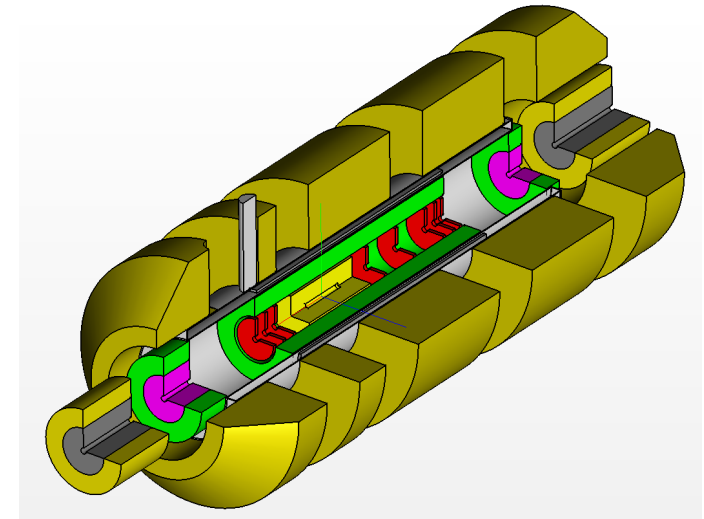
| Tracker (LHeC)                         | Fwd Tracker |                      |                   | Bwd Tracker          |                   | Total<br>(incl. Tab. 12.1) |
|--|-------------|----------------------|-------------------|----------------------|-------------------|----------------------------|
|  | pix         | pix <sub>macro</sub> | strip             | pix <sub>macro</sub> | strip             |                            |
| $\eta_{\text{max}}, \eta_{\text{min}}$ | 5.3, 2.6    | 3.5, 2.2             | 3.1, 1.6          | -4.6, -2.5           | -2.9, -1.6        | 5.3, -4.6                  |
| Wheels                                 | 2           | 1                    | 3                 | 2                    | 4                 |                            |
| Modules/Sensors                        | 180         | 180                  | 860               | 72                   | 416               | 10736                      |
| Total Si area [m <sup>2</sup> ]        | 0.8         | 0.9                  | 4.6               | 0.4                  | 1.8               | 40.7                       |
| Read-out-Channels [10 <sup>6</sup> ]   | 404.9       | 68.9                 | 26.4              | 27.6                 | 10.6              | 2934.2                     |
| pitch <sup>r-φ</sup> [μm]              | 25          | 100                  | 100               | 100                  | 100               |                            |
| pitch <sup>z</sup> [μm]                | 50          | 400                  | 50k <sup>2)</sup> | 400                  | 10k <sup>1)</sup> |                            |
| Average $X_0/\Lambda_I$ [%]            | 6.7 / 2.1   |                      |                   | 6.1 / 1.9            |                   |                            |
| incl. beam pipe [%]                    |             |                      |                   |                      |                   | 40 / 25                    |





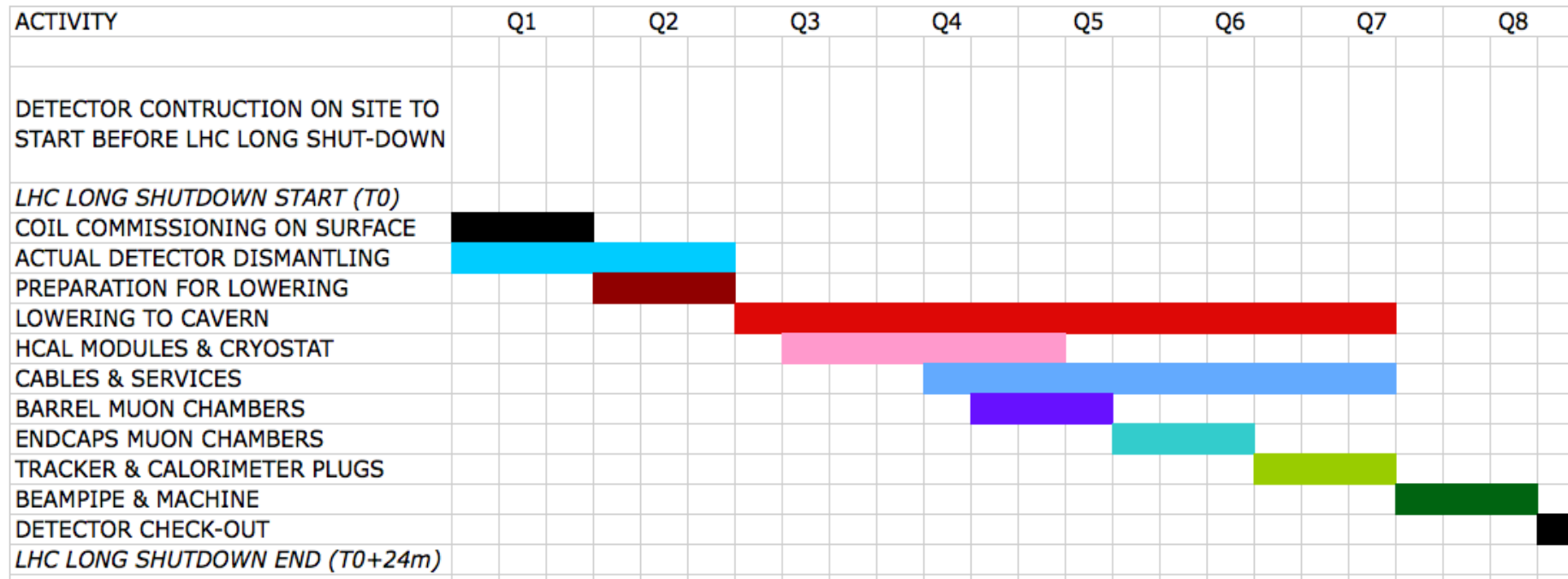
Detector fits in L3 magnet support

# Installation Study



Modular structure

## LHeC INSTALLATION SCHEDULE



Detector Installation possible within about two-years shutdown: pre-mounting on surface

# Integration of eA and AA Detector Concepts

Could one merge the LHeC (2007.14491) and a novel Heavy Ion detector (“A3”, 1902.01211) concepts ?



# What we can learn in an ep/eA collider

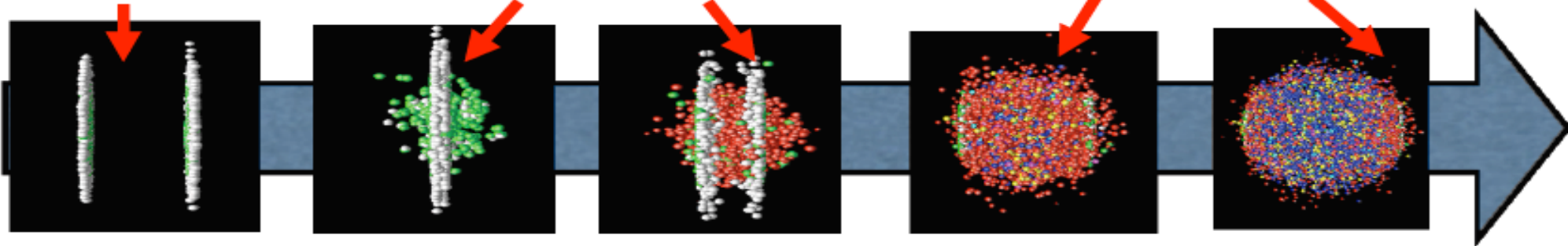
We do not have a **QUANTITATIVE** understanding of the nuclear behaviour

required for A-A and QGP studies

The colliding objects

Early stages

Analyzing the medium



Gluons from saturated nuclei → Glasma? → QGP → Reconfinement

Dense regime: lack of information about

- small-x partons
- correlations
- transverse structure

Particle production at the very beginning:

- Which factorization?
- How can a system behave as isotropised so fast?

Probing the medium through energetic particles:

- Dynamical mechanisms for opacity
- How to extract accurately medium parameters?

ep and eA:

- nuclear WF & PDFs
- mechanism of particle production
- tomography

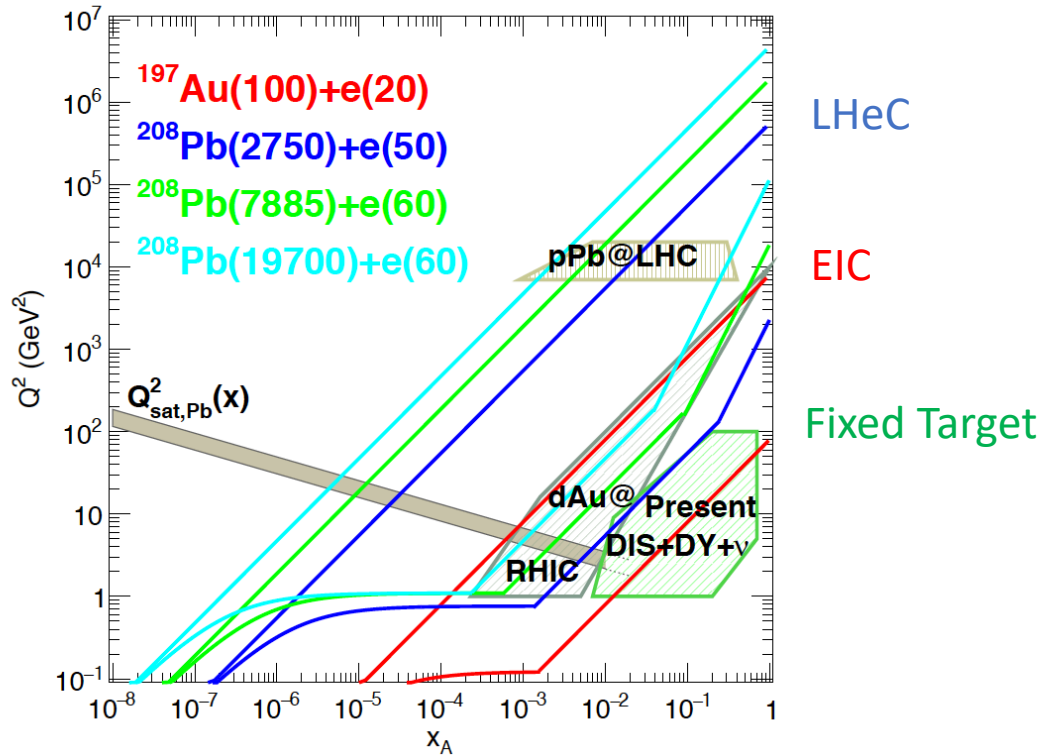
ep and eA:

- initial conditions for plasma formation
- how small can a system be and still show collectivity?

ep and eA:

- modification of radiation and hadronization in the nuclear medium
- initial effects on hard probes

# Partons in Nuclei

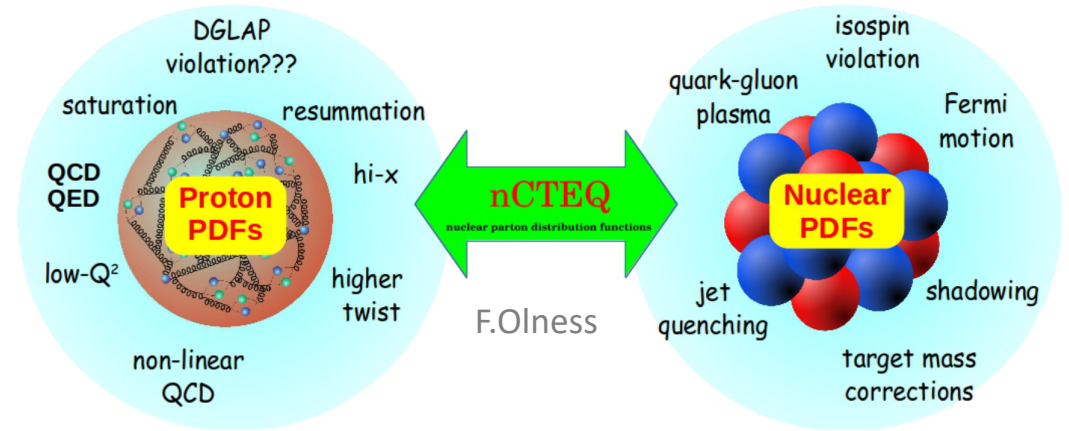


## Direct measurements of R:

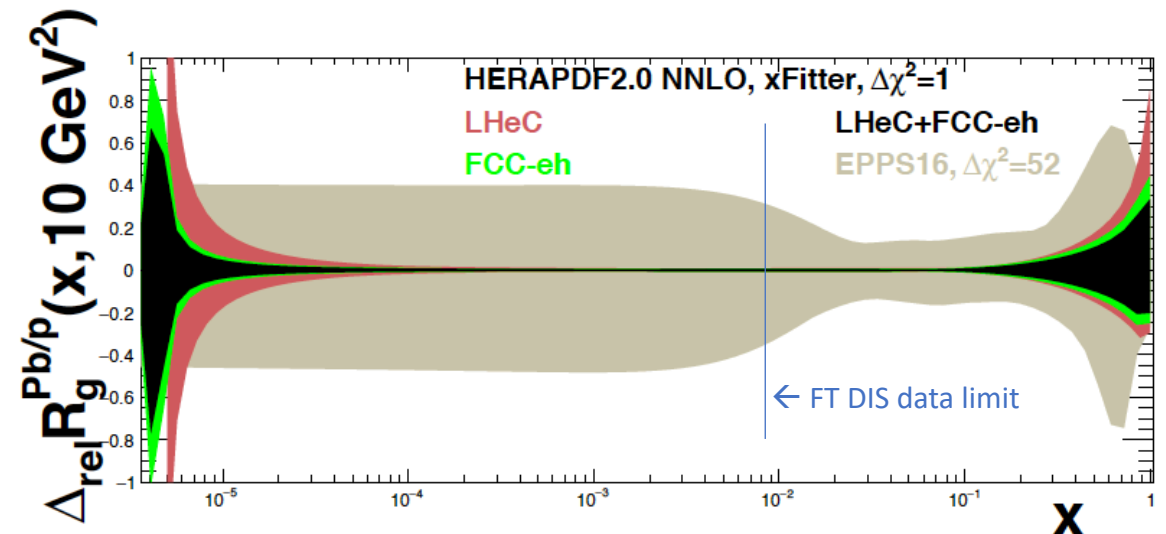
$$R_i(x, Q^2) = \frac{f_i^A(x, Q^2)}{A f_i^p(x, Q^2)}, \quad i = u, d, s, c, b, g, \dots$$

Resolution of complete quark and gluon structure (NC+CC)  
 Disentanglement of nuclear + parton dynamic effects  
 Deep into saturation region with small strong coupling (pQCD)

## Complexity of (de) confinement in proton and nuclei



## Direct determination of $R_g$ with proton and lead data, full error



## New paradigm: small systems

Totally unexpected:

the discovery of correlations –ridge, flow- in small systems **pA & pp**

- Smooth continuation of heavy ion phenomena to small systems and low density
- **Small systems as pA and pp show QGP-like features**

Two serious contenders remain today:

- **initial state:** quantum correlations as calculated by CGC
- **final state:** interactions leading to collective flow described with hydrodynamics => **equilibration?**

The **old paradigm** that

- we study hot & dense matter properties in heavy ion **AA** collisions
- cold nuclear matter modifications in **pA**
- and we use **pp** primarily as comparison data **appears no longer sensible**

We should examine a **new paradigm**, where the physics underlying soft collective signals can be the same in all high energy reactions, **from  $e^+e^-$  to central AA**

Joint eA/ep and pp/pA/AA physics in a common apparatus is probably an ideal for new heavy ion physics to very high precision.

A common/dual/joint - you name it- experiment would have unprecedented reach into physics

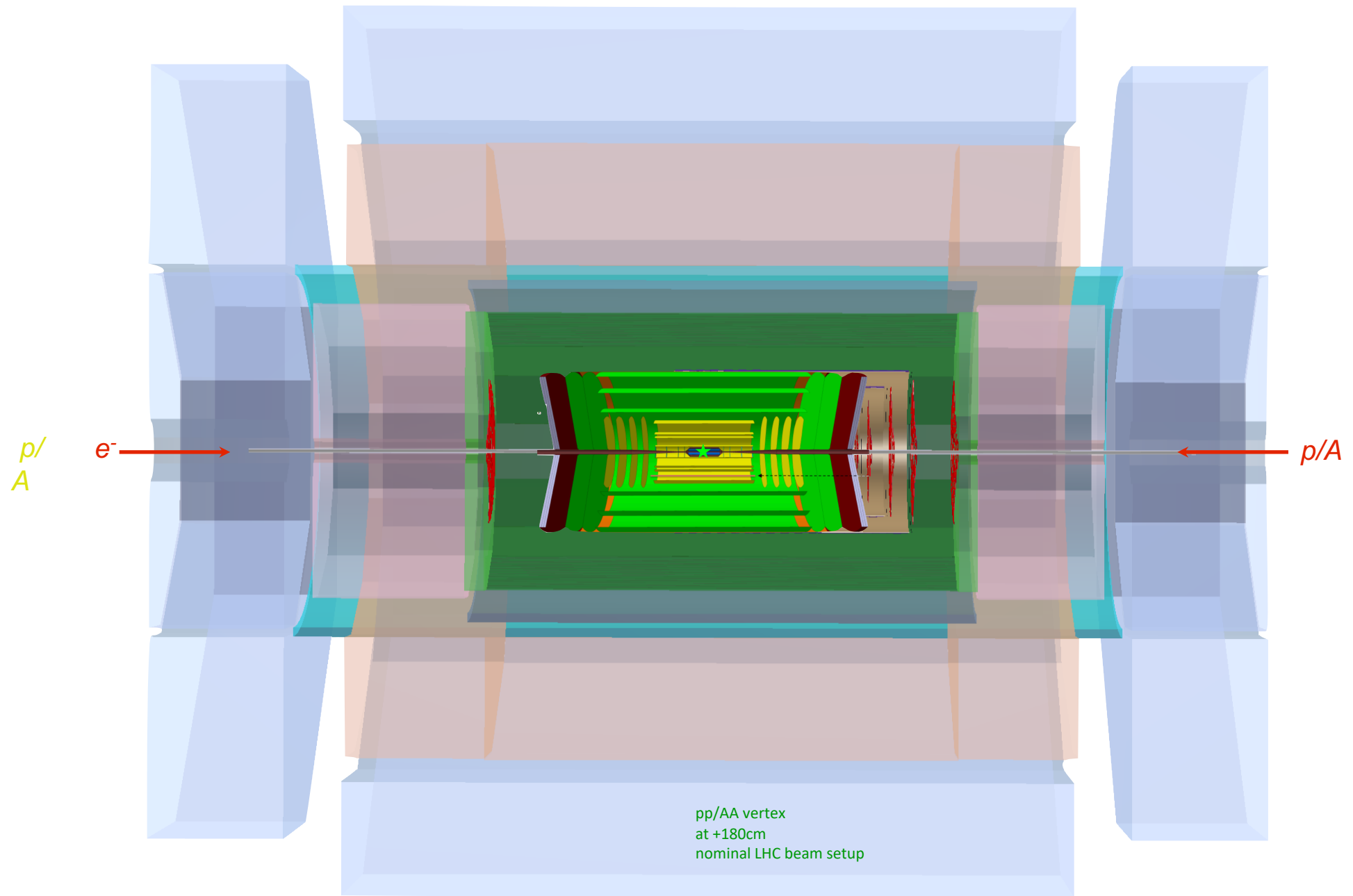
AA

from low  $p_T$ , to quarkonia + hard scales

eA

DIS extended by 3-4 orders of magnitude.

Invites new and further thinking, and to carefully evaluate gains and drawbacks of such an enterprise.



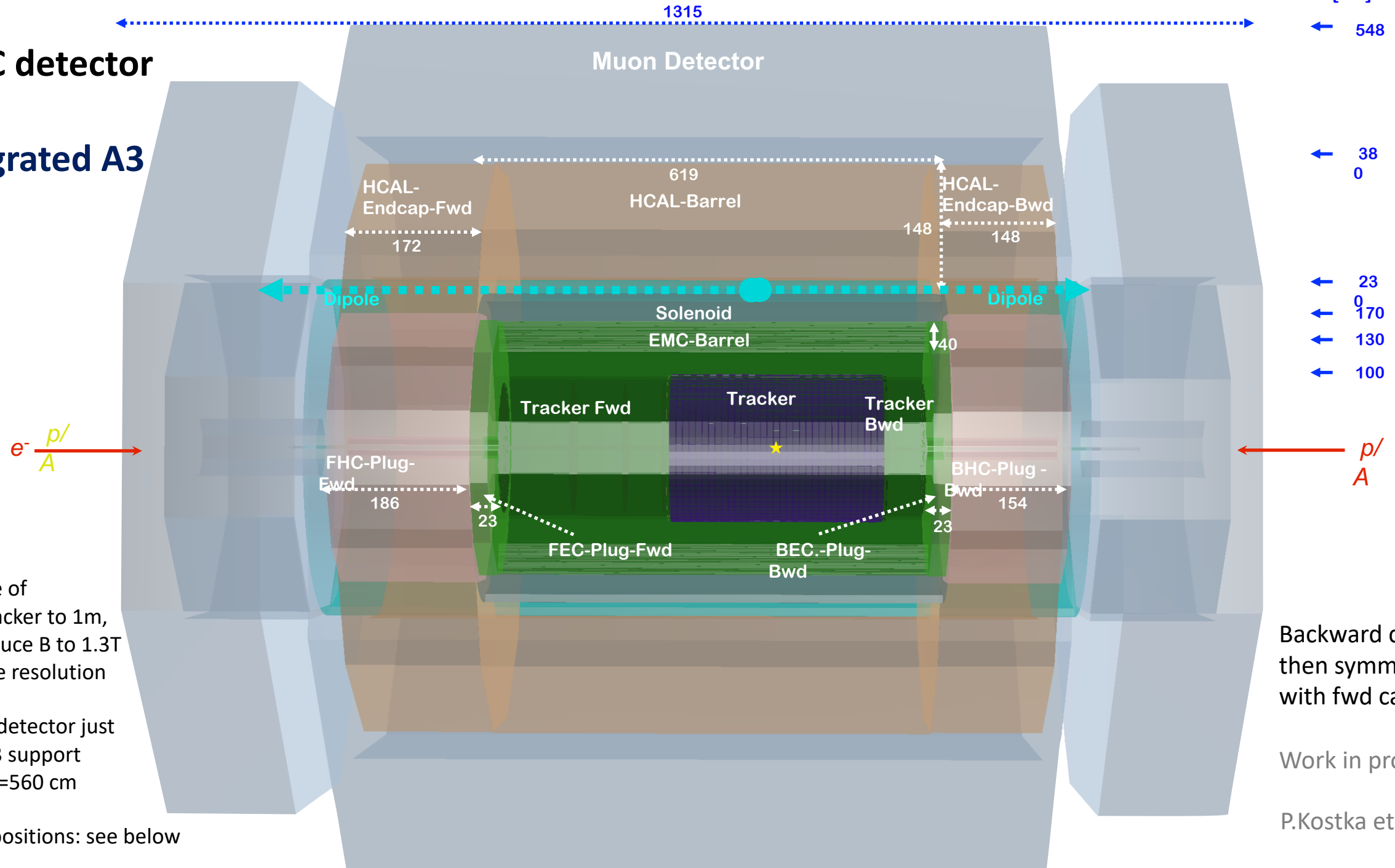
$p/A$

$e^-$

$p/A$

pp/AA vertex  
at +180cm  
nominal LHC beam setup

# LHeC detector with integrated A3



Increase of radii, tracker to 1m, may reduce B to 1.3T for same resolution

Overall detector just fits in L3 support  
 $R_{free}(L3)=560$  cm

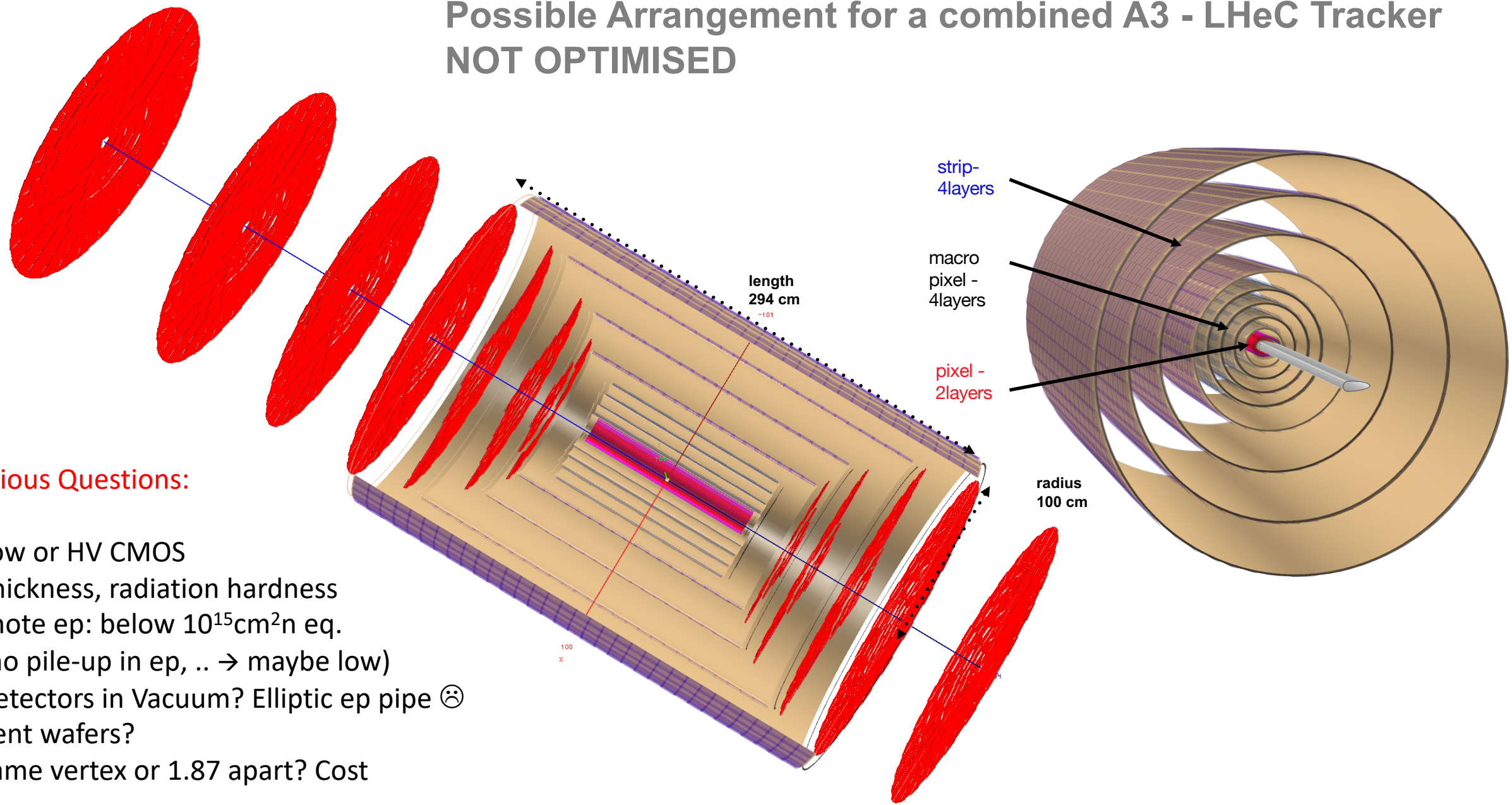
Vertex positions: see below

Backward calos then symmetric with fwd calos

Work in progress

P.Kostka et al.

# Possible Arrangement for a combined A3 - LHeC Tracker NOT OPTIMISED



## Various Questions:

- Low or HV CMOS
- Thickness, radiation hardness (note ep: below  $10^{15} \text{cm}^2 \text{n eq.}$  no pile-up in ep, ..  $\rightarrow$  maybe low)
- Detectors in Vacuum? Elliptic ep pipe ☹️
- Bent wafers?
- Same vertex or 1.87 apart? Cost
- ...

# Questions and Tentative Comments on Merger

Initial thoughts and questions: LHeC Meeting 29.10.

and tentative answers 23.11.20

## First derived questions:

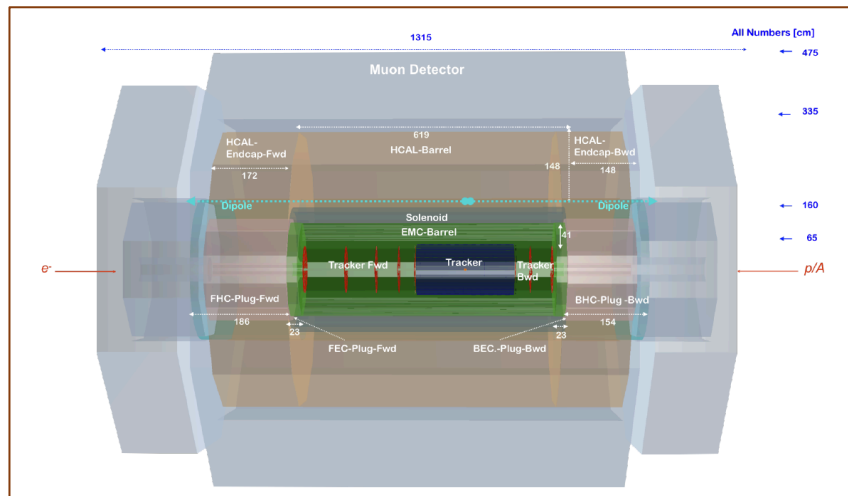
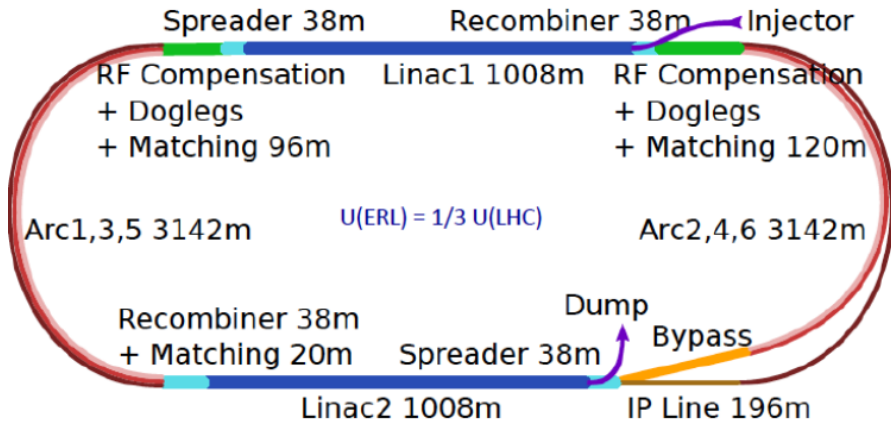
- Can we generate luminosity at 0 and +1.8m for pp/AA and ep/eA, respectively? **yes, time needed sharing**
- How does LHeC detector change if we integrate A3 into LHeC **extension in radius, B reduced, low V CMOS, ..**
- How would A3 detector change? Would it profit from the ep detector environment?  
Muons, calorimetry? **Better answered with A3 insight, one would expect this leads to a hard scale program**
- How does the physics potential change? **eA programme at TeV scales. LHeC is most powerful EIC one can build**

## Detailed Questions

- Magnetic fields: solenoid: if we go to half our value, and enlarge the radius by 2, we gain factor 2 resolution **ok**  
Dipole: the dipole (and solenoid) would move further out, any problem? **Rather not. Note low material magnets**
- Choice of Silicon technology for IT, are we compatible with them? Probably yes. **low V CMOS probably ok for LHeC**
- Readout and Trigger: speed, data volume, 2 trigger and r/o branches or 1 etc. **To be studied**
- For their design the extended ep beam pipe is a nuisance (as it is for ours) --> place Si inside pipe?? **challenging**
- There are many more..

→ It indeed seems feasible to combine the two detectors and IR concepts (further machine studies ongoing)

# Concluding Remarks



This is indeed **affordable** - O(1) billion CHF for another TeV collider

It **sustains the HL-LHC** and exploits this massive O(5) BCHF investment

**Physics: Unique:** Microscope of substructure (not resolved!), empowers LHC searches and Higgs measurements challenging  $e^+e^-$ , Discovery in electroweak and strong i.a. sector, Revolution of HI physics

**Technology:** Accelerator: highest energy ERL application - green. Detector: exciting place for new technology (CMOS, timing, thin calo.. etc) in classic DIS, low radiation environment, no pileup. Exciting place also for known technology to reappear and work.

**Merging LHeC with A3** resolves conceptual conflict on IP2 and promises to lead to new chapter of HI and accelerator physics (tentative)

**Next steps:** PERLE facility at Orsay, considerations for a detector proposal to LHCC, embedded and subject to CERN's future, which is also related to that of the CEPC.

The LHeC group believes that **diversity** (at the energy frontier too) **is key** to help particle physics theory to restore its predictive power..



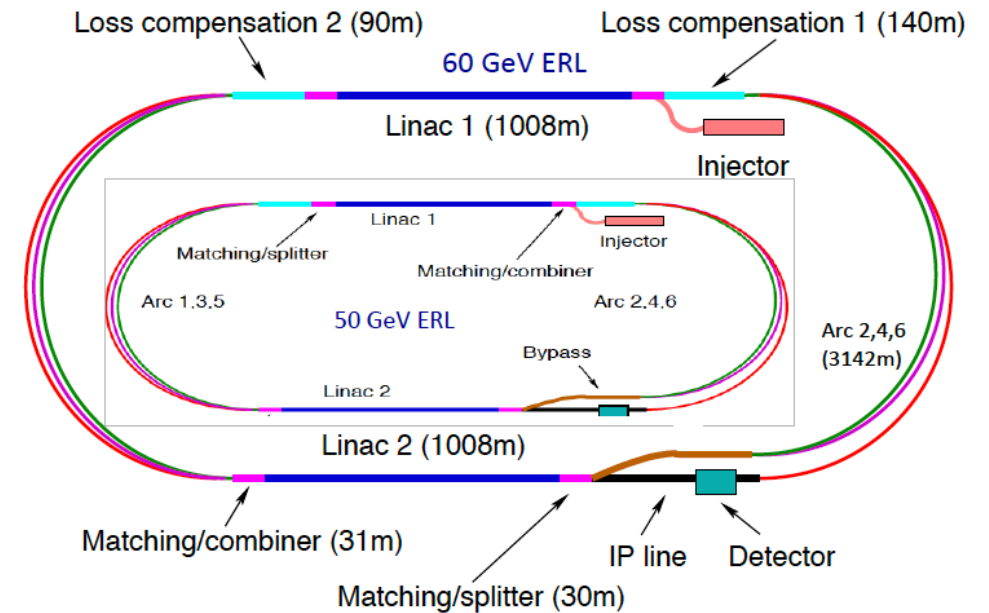
backup

# The ERL in more Detail

| Parameter  | Unit          | Value          |
|--|---------------|----------------|
| Injector energy                                    | GeV           | 0.5            |
| Total number of linacs                             |               | 2              |
| Number of acceleration passes                      |               | 3              |
| Maximum electron energy                            | GeV           | 49.19          |
| Bunch charge                                       | pC            | 499            |
| Bunch spacing                                      | ns            | 24.95          |
| Electron current                                   | mA            | 20             |
| Transverse normalized emittance                    | $\mu\text{m}$ | 30             |
| Total energy gain per linac                        | GeV           | 8.114          |
| Frequency  | MHz           | 801.58         |
| Acceleration gradient                              | MV/m          | 19.73          |
| Cavity iris diameter                               | mm            | 130            |
| Number of cells per cavity                         |               | 5              |
| Cavity length (active/real estate)                 | m             | 0.918/1.5      |
| Cavities per cryomodule                            |               | 4              |
| Cryomodule length                                  | m             | 7              |
| Length of 4-CM unit                                | m             | 29.6           |
| Acceleration per cryomodule (4-CM unit)            | MeV           | 289.8          |
| Total number of cryomodules (4-CM units) per linac |               | 112 (28)       |
| Total linac length (with with spr/rec matching)    | m             | 828.8 (980.8)  |
| Return arc radius (length)                         | m             | 536.4 (1685.1) |
| Total ERL length                                   | km            | 5.332          |

Table 10.1: Parameters of LHeC Energy Recovery Linac (ERL).

**Positrons:** 500pC is  $3 \cdot 10^9 e^-/\text{bunch} \rightarrow 20\text{mA}$  and  $1.2 \cdot 10^{17} e^-/\text{s}$   
 LHeC programme needs  $e^-p$  predominantly (Higgs) and only smaller  $e^+p$  sample,  $\sim \text{fb}^{-1} \rightarrow O(10^{15}) e^+/\text{s}$ , still demanding!



- LHeC Configuration reduced from 60 to 50 GeV.
- LINAC: 112 cryomodules with 4 cavities each  
 $\rightarrow$  Total number of cavities: 896 [ILC:  $O(10^4)$ ]
- Configuration may be staged with less RF
- Tunnel is small part of cost and better not reduced further, synchrotron loss, upgrades..
- ERL reduces power to  $\ll \text{GW}$  and dumps at  $< \text{GeV}$   
 $\rightarrow$  novel, "green" accelerator technology

# Machine Parameters and Operation - ep

arXiv:2007.14401

| Parameter    | Unit                                  | LHeC |       |       |           | FCC-eh       |              |
|--------------|---------------------------------------|------|-------|-------|-----------|--------------|--------------|
|              |                                       | CDR  | Run 5 | Run 6 | Dedicated | $E_p=20$ TeV | $E_p=50$ TeV |
| $E_e$        | GeV                                   | 60   | 30    | 50    | 50        | 60           | 60           |
| $N_p$        | $10^{11}$                             | 1.7  | 2.2   | 2.2   | 2.2       | 1            | 1            |
| $\epsilon_p$ | $\mu\text{m}$                         | 3.7  | 2.5   | 2.5   | 2.5       | 2.2          | 2.2          |
| $I_e$        | mA                                    | 6.4  | 15    | 20    | 50        | 20           | 20           |
| $N_e$        | $10^9$                                | 1    | 2.3   | 3.1   | 7.8       | 3.1          | 3.1          |
| $\beta^*$    | cm                                    | 10   | 10    | 7     | 7         | 12           | 15           |
| Luminosity   | $10^{33} \text{cm}^{-2}\text{s}^{-1}$ | 1    | 5     | 9     | 23        | 8            | 15           |

**Table 2.3:** Summary of luminosity parameter values for the LHeC and FCC-eh. Left: CDR from 2012; Middle: LHeC in three stages, an initial run, possibly during Run 5 of the LHC, the 50 GeV operation during Run 6, both concurrently with the LHC, and a final, dedicated, stand-alone  $ep$  phase; Right: FCC-eh with a 20 and a 50 TeV proton beam, in synchronous operation.

No pileup

For comparison, HERA I operated at  $10^{31}\text{cm}^{-2}\text{s}^{-1}$ , and was upgraded by a factor of up to 4 for HERA II. The total luminosity delivered was  $1 \text{fb}^{-1}$  over a running period of 15 years, including shutdowns. LHeC may operate at  $20 \times 1000 \text{GeV}^2$  and "repeat" all of HERA in a short running period.

The initial CDR considers a Ring-Ring  $ep$  collider as a back-up solution. May be revived for HE-LHC.

# Machine Parameters - eA

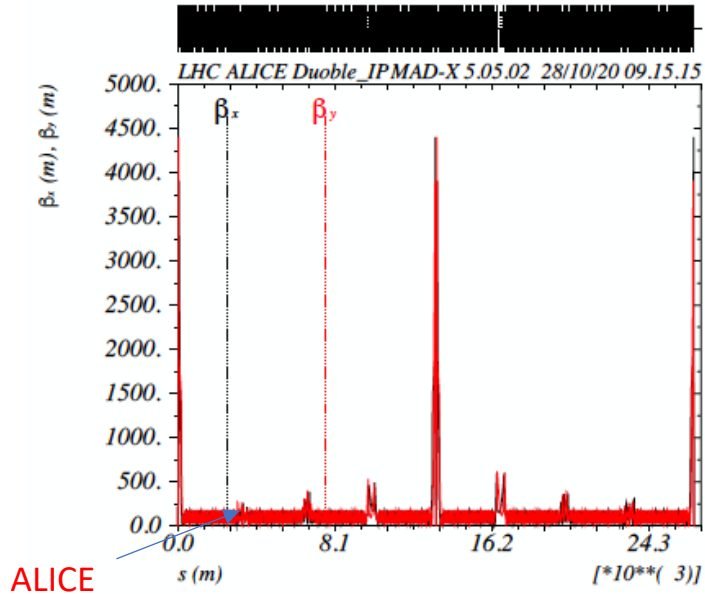
| Parameter                            | Unit                                 | LHeC  | FCC-eh<br>( $E_p=20$ TeV) | FCC-eh<br>( $E_p=50$ TeV) |
|--------------------------------------|--------------------------------------|-------|---------------------------|---------------------------|
| Ion energy $E_{Pb}$                  | PeV                                  | 0.574 | 1.64                      | 4.1                       |
| Ion energy/nucleon $E_{Pb}/A$        | TeV                                  | 2.76  | 7.88                      | 19.7                      |
| Electron beam energy $E_e$           | GeV                                  | 50    | 60                        | 60                        |
| Electron-nucleon CMS $\sqrt{s_{eN}}$ | TeV                                  | 0.74  | 1.4                       | 2.2                       |
| Bunch spacing                        | ns                                   | 50    | 100                       | 100                       |
| Number of bunches                    |                                      | 1200  | 2072                      | 2072                      |
| Ions per bunch                       | $10^8$                               | 1.8   | 1.8                       | 1.8                       |
| Normalised emittance $\epsilon_n$    | $\mu\text{m}$                        | 1.5   | 1.5                       | 1.5                       |
| Electrons per bunch                  | $10^9$                               | 6.2   | 6.2                       | 6.2                       |
| Electron current                     | mA                                   | 20    | 20                        | 20                        |
| IP beta function $\beta_A^*$         | cm                                   | 10    | 10                        | 15                        |
| e-N Luminosity                       | $10^{32}\text{cm}^{-2}\text{s}^{-1}$ | 7     | 14                        | 35                        |

**Table 2.4:** Baseline parameters of future electron-ion collider configurations based on the electron ERL, in concurrent  $eA$  and  $AA$  operation mode with the LHC and the two versions of a future hadron collider at CERN. Following established convention in this field, the luminosity quoted, at the start of a fill, is the *electron-nucleon* luminosity which is a factor  $A$  larger than the usual (i.e. electron-nucleus) luminosity.

arXiv:2007.14401

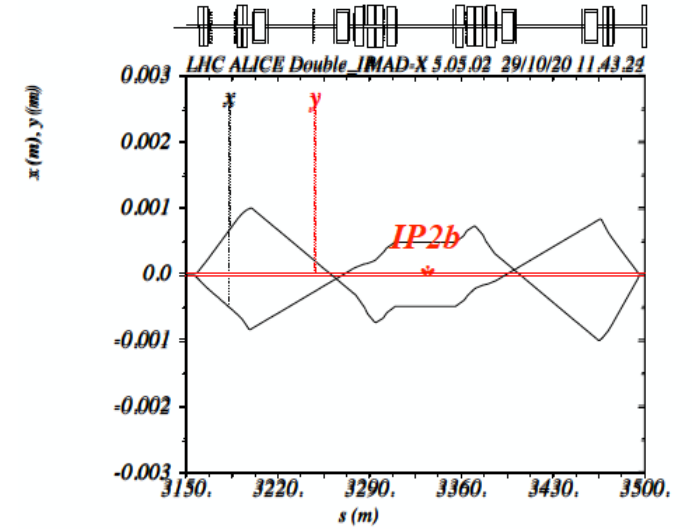
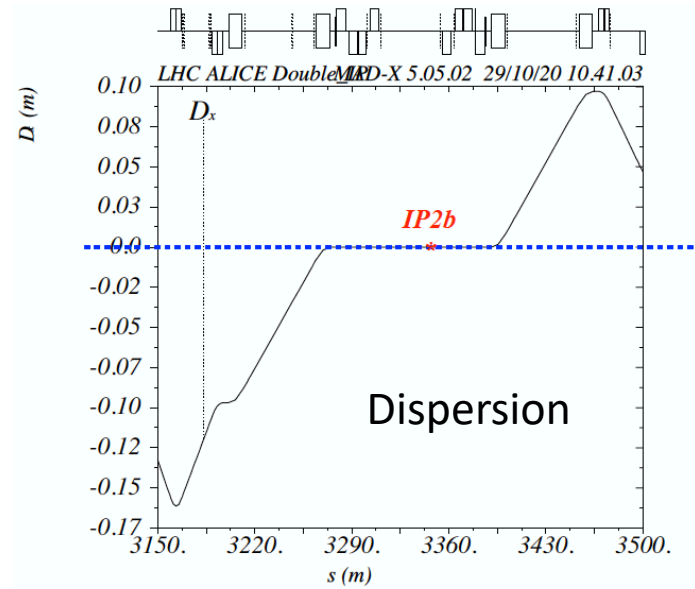
The LHeC and FCC-eh are the highest energy, most powerful electron-ion colliders the world may build. Saturation, Parton Dynamics and Structure in Nuclei, Quarkonia, Jets, Tomography of p and Nuclei, ..

# Optics for IP2

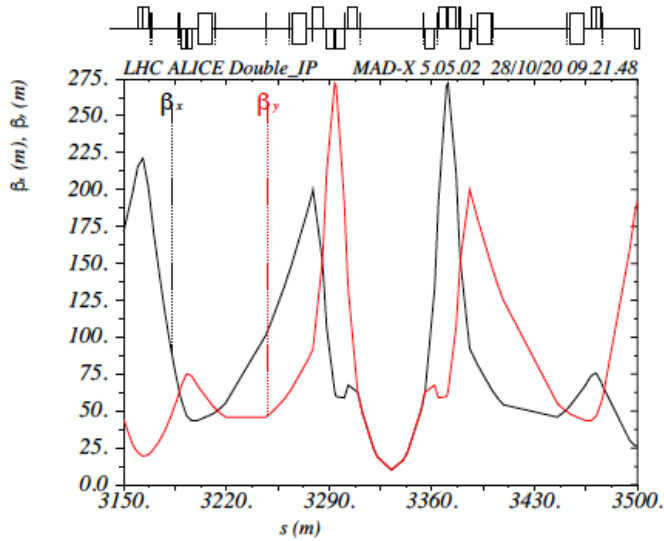


LHC Optics – beta vs path

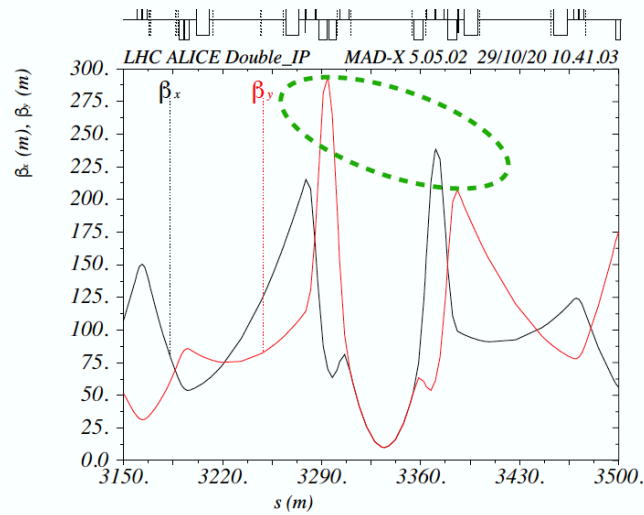
ALICE



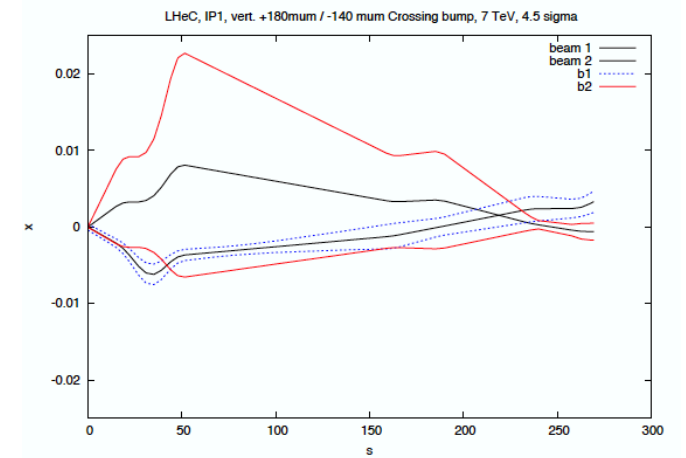
Separation bump (std LHC procedure)



ALICE Luminosity Optics  $\beta_x^* = 10\text{m}$



ALICE Luminosity Optics: IP2b=1.87m



Shift in time and vertical xing 140mrad

→ No showstopper for ep and AA

# Aperture Staggered Quadrupoles

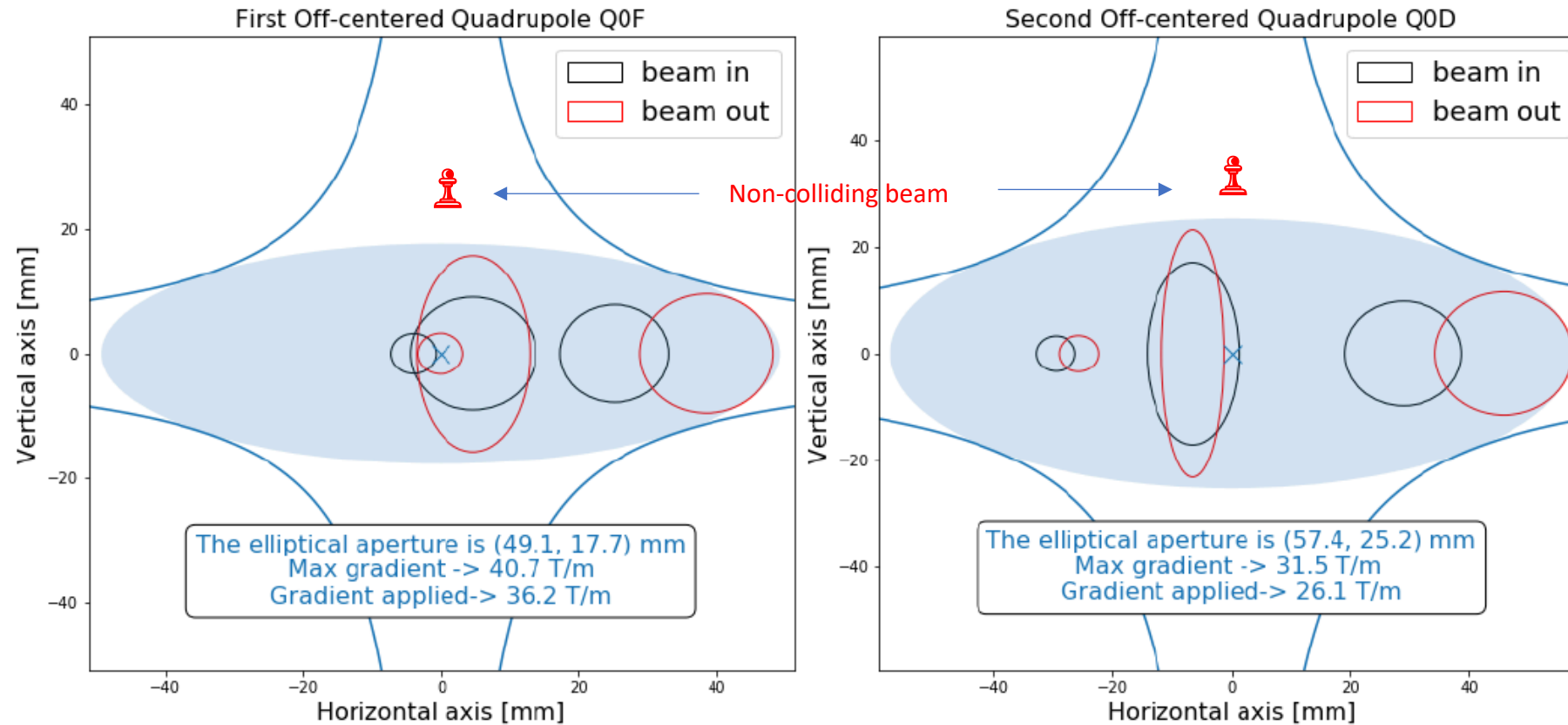


**Figure 10.42:** The position of the three beams at the entrance (black) and exit (red) of the electron doublet magnets. Following the internal convention,  $15\sigma$  plus 20% beta beating plus 2mm orbit tolerances beam envelopes are chosen for the proton beams. The beam size of the electrons refer to  $20\sigma$ . From left to right the three beams are respectively the non colliding proton beam (tiny circles), electron beam (squeezed ellipses) and the colliding proton beam.

# Aperture Half-Quadrupole

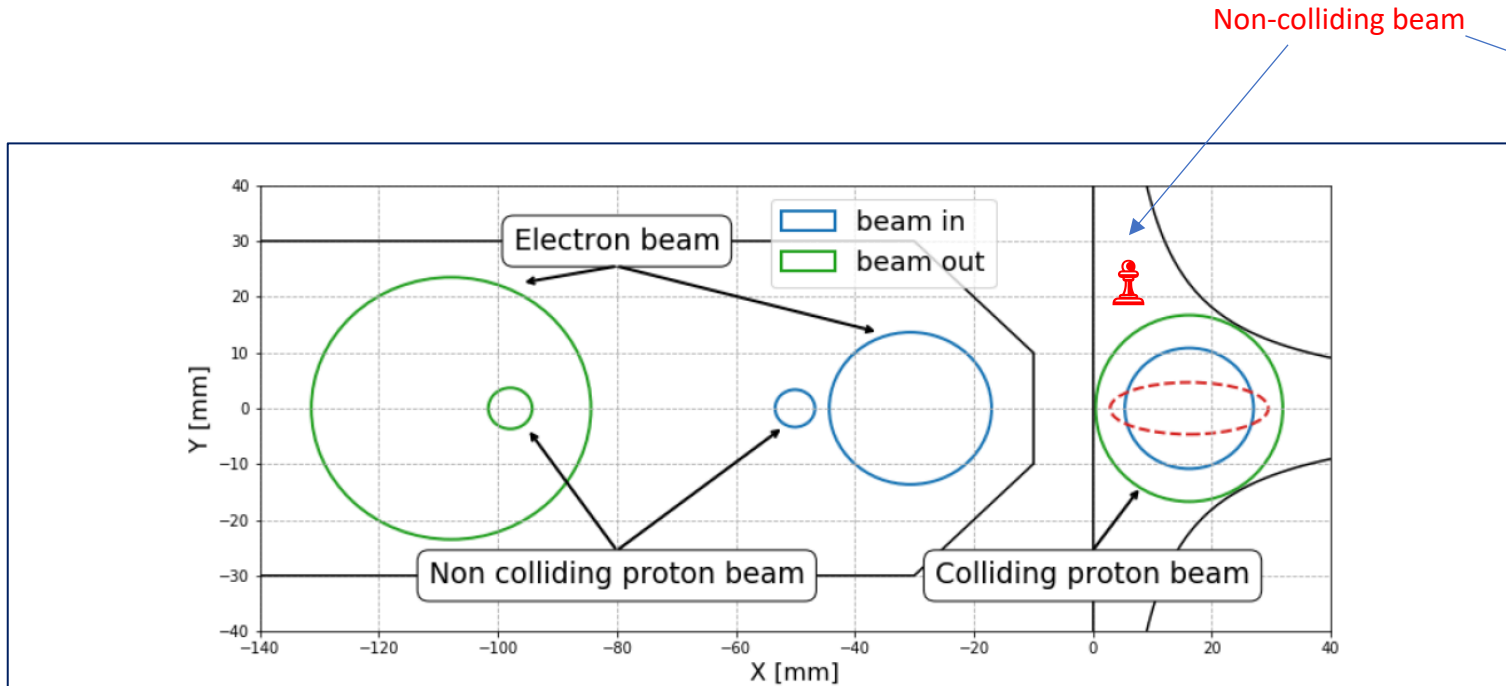
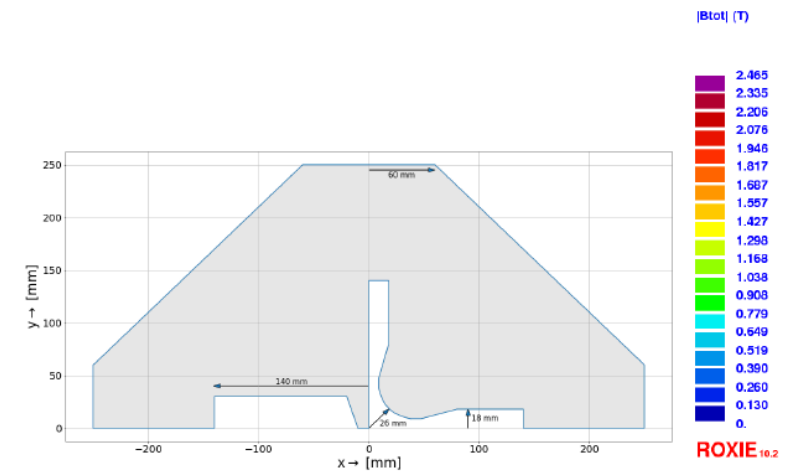
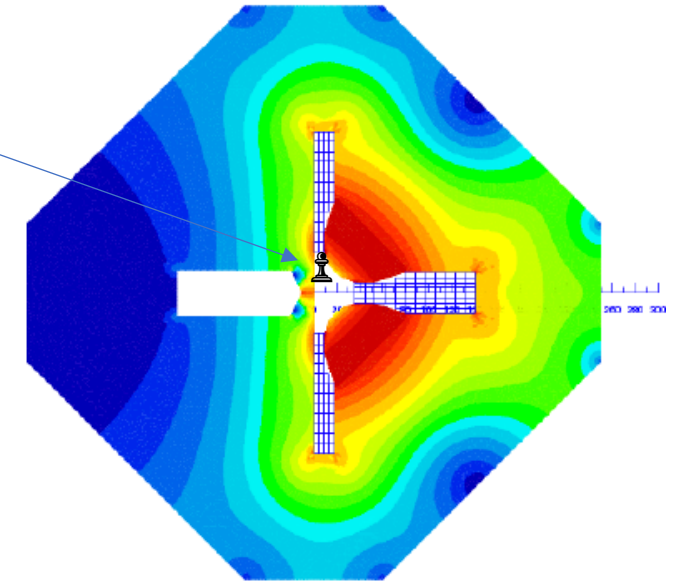


**Figure 10.41:** The position of the three beams at the entrance (blue) and exit (green) of the half quadrupole. The colliding proton beam is centered inside the main magnet aperture, while the second proton beam and the electrons are located in the field free region. The dashed red line represents the injection proton beam at the output of the half quadrupole.



# Q1 and further Quadrupoles

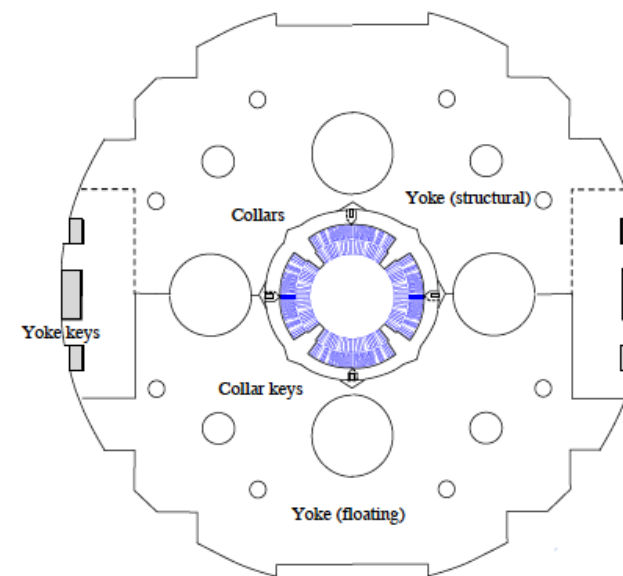
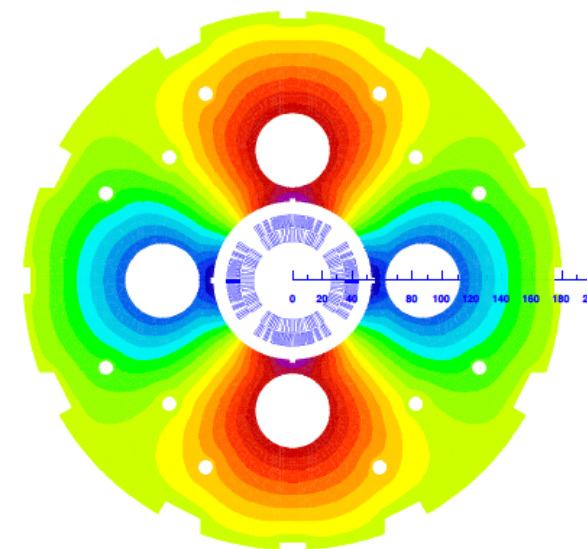
| Magnet parameter                           | Unit | Magnet type |         |                    |                    |
|--|------|-------------|---------|--------------------|--------------------|
|  |      | Q1A         | Q1B     | Q2 type            | Q3 type            |
| Superconductor type                        |      | Nb-Ti       | Nb-Ti   | Nb <sub>3</sub> Sn | Nb <sub>3</sub> Sn |
| Coil aperture radius $R$                   | mm   | 20          | 32      | 40                 | 45                 |
| Nominal current $I_{\text{nom}}$           | A    | 7080        | 6260    | 7890               | 9260               |
| Nominal gradient $g$                       | T/m  | 252         | 164     | 186                | 175                |
| Percentage on the load line                | %    | 78          | 64      | 71                 | 75                 |
| Beam separation distance $S_{\text{beam}}$ | mm   | 106-143     | 148-180 | 233-272            | 414-452            |

**Table 10.28:** Main triplet magnet parameters

Q2, Q3 desirably NOT Nb<sub>3</sub>Sn but Nb-Ti as suggested by current experience

B Holzer, S Russenschuck

Aperture of Q1A needs study, when non-colliding p beam is kept in vacuum





# Energy Recovery and Synergies

LHeC/FCC-eh: high luminosity, high energy  
→ High ERL power facility  $P = I_e E_e$

**This is a programme for high quality SRF ( $Q_0 > 10^{10}$ ), high current sources, and multiturn to reach high  $E_e$**

## **Future/current ERL developments: distribution of emphasis**

- CBETA: high current, single turn - for e cooler (EIC)
- MESA: polarised beam - for new PV asymmetry exp.
- CEBAF: few GeV energy - for study of syn. radiation
- PERLE: high current, multiturn - for exp's and future

Plans: Daresbury, Darmstadt, Berlin. Revival of KEK ERL normal conducting ERL machine at BINP

Coordination: Lab Director Group (A Stocchi JLab for ERL)  
European Accelerator R+D Roadmap: CERN council 9/21  
ERL Network. ERL workshop series

## **Technical Synergies of LHeC with other applications**

- SAPPHIRE: a  $\gamma\gamma$  collider : Higgs, eweak and QCD machine  
F. Zimmermann et al, arXiv:1208.2827
- Racetrack as an injector into FCC-ee [direct into Z]  
O. Bruening, Y. Papaphilippou
- LHeC-FEL  
F. Zimmermann et al, work in progress
- Injector into FCC-hh  
R. Calaga
- Proposal of ERL Version of FCC-ee for high Lumi at high  $E_e$   
V Litvinenko, T Roser, M Chamizo-Llatas arXiv: 1909.04437
- 802 MHz technology: PERLE, FCC-ee, eSPS  
F Marhauser, B Rimmer et al
- 704 MHz SPL Cryomodule (CERN) modified for PERLE  
F Gerigk, E Jensen et al.
- ALICE (Daresbury) Gun delivered to Orsay for PERLE  
D Angal-Kalinin, B Militsyn et al
- JLEIC Booster (Jlab) likely to be used in PERLE  
F Hannon, B Rimmer et al
- Forward Calorimetry: FCC-hh and ee colliders / CALICE..
- Inner Tracker/CMOS: ee colliders, new HI detector at IP2
- ....

# Partonic evolution and hadronization

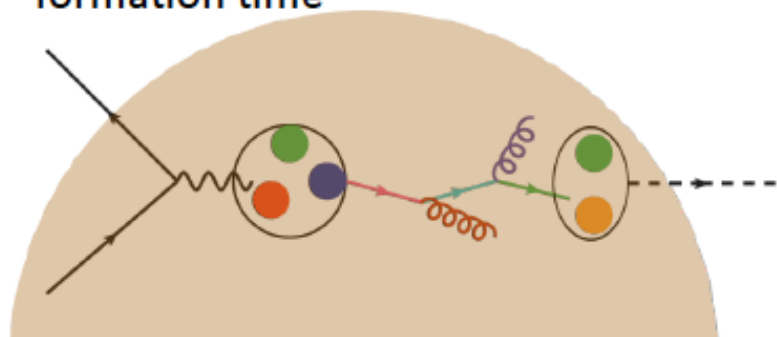
Relevant for particle production and QGP analysis in HIC:

jets plentiful in eA  
benchmark for jet quenching studies in AA

Low energy:

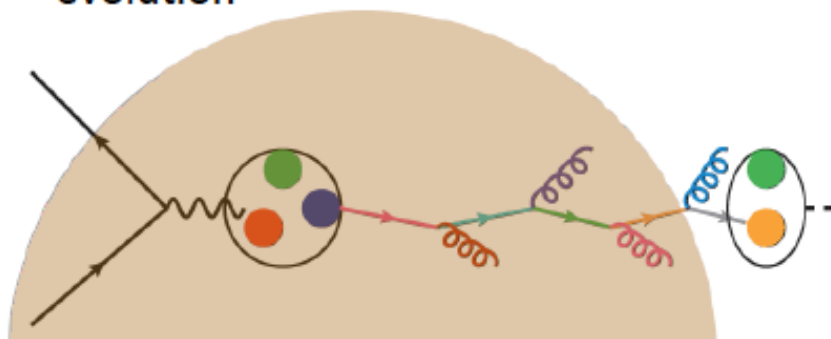
hadronization in matter

- (pre)hadronic absorption
- formation time

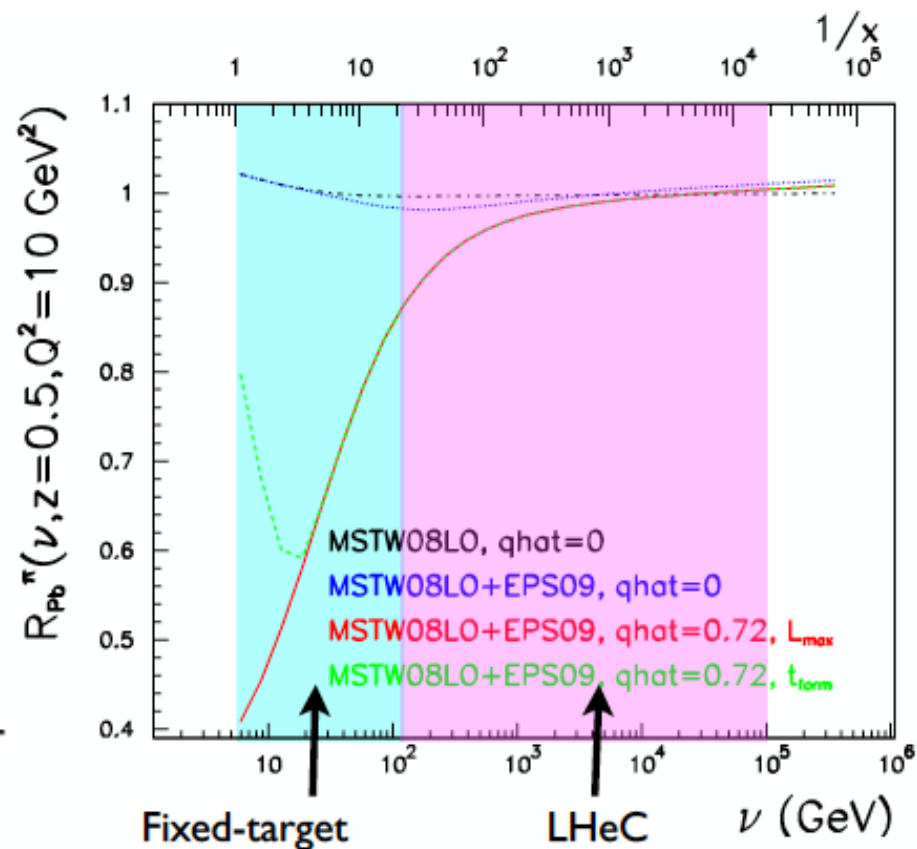


High energy:

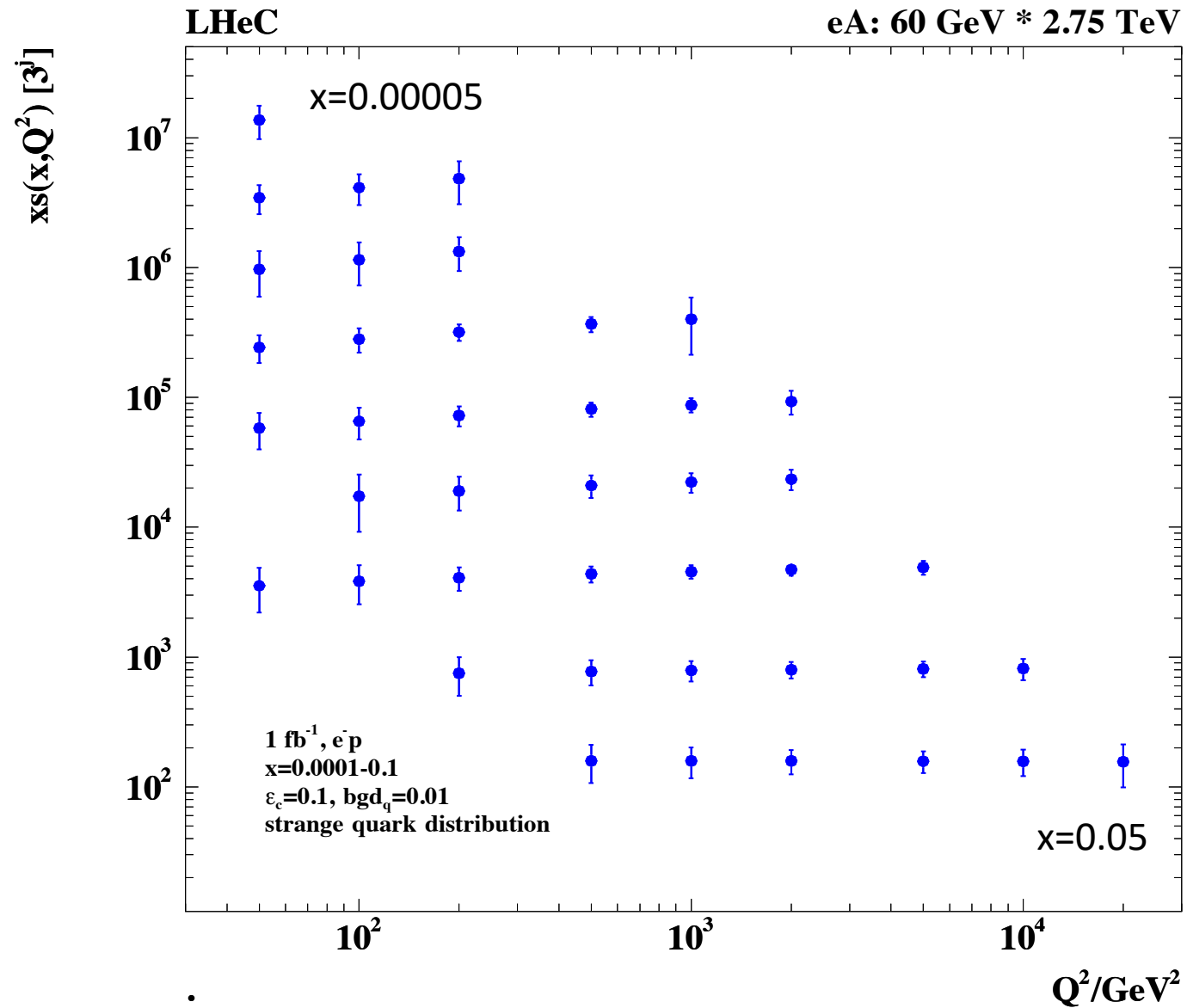
- modification of partonic evolution



Ratio of fragmentation functions Pb/p



# Heavy Flavour – Strange in ePb - from CC



# Other possible studies: quarkonium production

## Production mechanism and polarization:

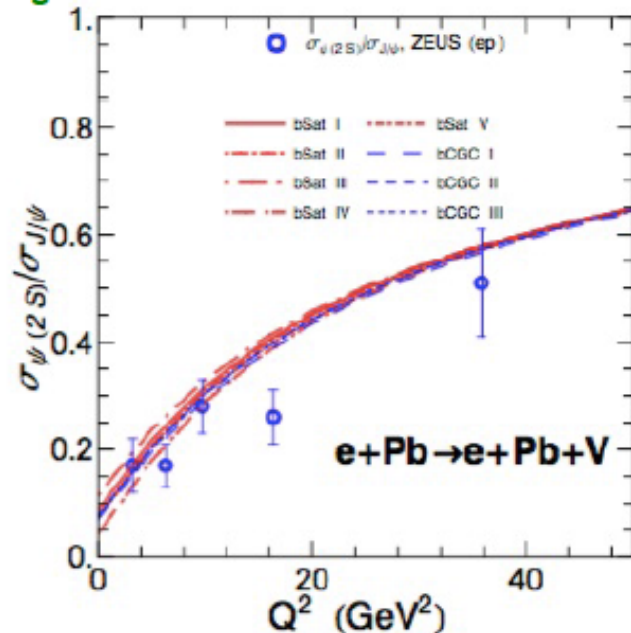
polarized  $J/\psi$  photoproduction can be studied more precisely and up to much larger values of  $p_T$  in **ep @ LHeC**

⇒ test NRQCD factorization in charmonium physics

Butenschoen Kniehl

**Charmonium WF** in diffractive DIS within the dipole formalism

Cheng et al.



## Spatial and Momentum Tomography of Hadrons and Nuclei

**Gluon TMDs** could be directly probed by looking at  $p_T$  distributions and azimuthal asymmetries in  $e p \rightarrow e Q \bar{Q} X$

Boer, Lansberg, Pisano

## Gluon GPDs

$\Upsilon$  production at an EIC to determine the gluon density transverse spatial profiles in a wide range of  $x$  and consequently provide a path to determine the gluonic radius of the nucleon and the contribution of the total angular momentum of gluons to the nucleon spin

Joosten and Meiziani

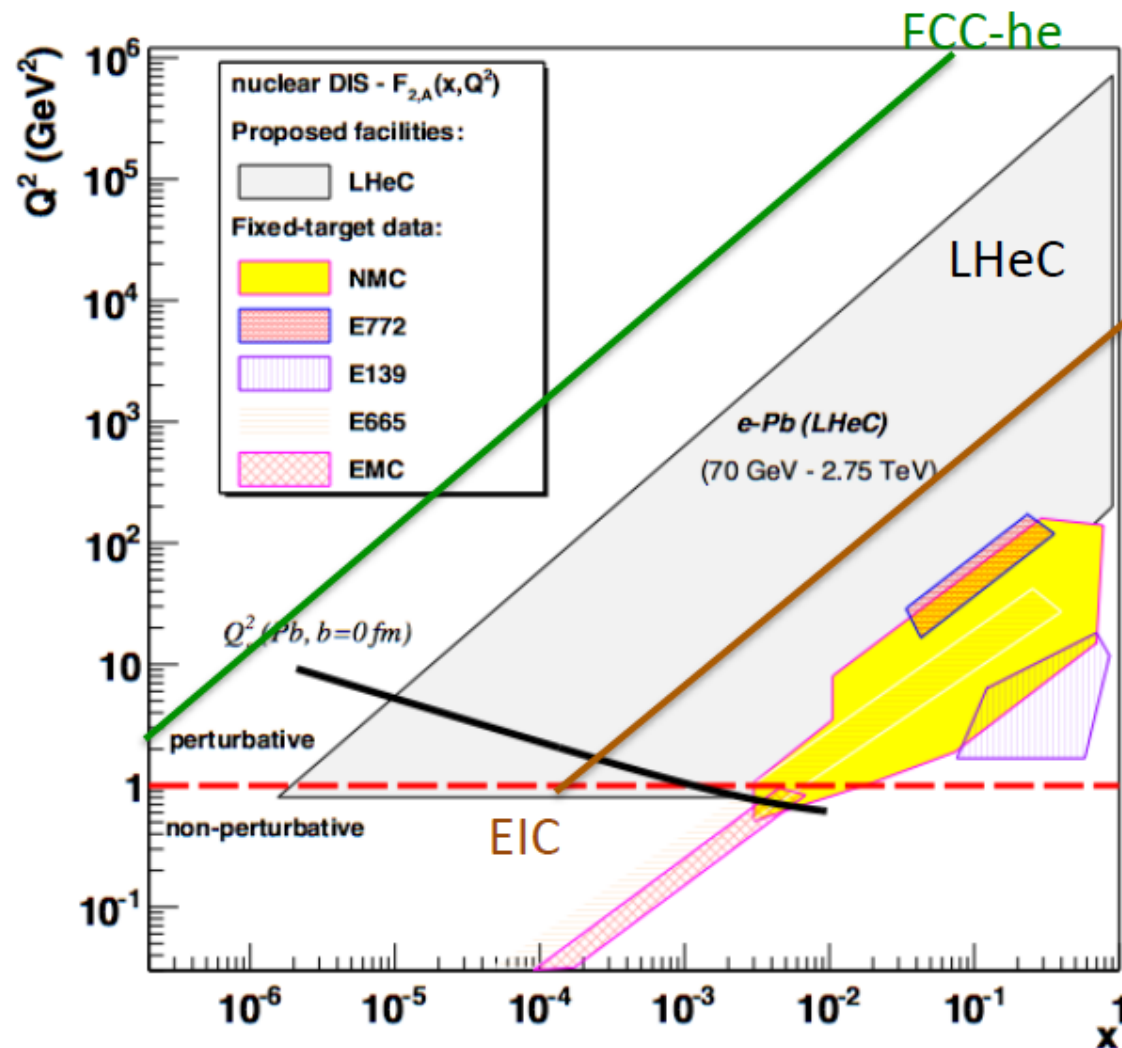
# Kinematic Ranges of IA DIS – Past and Future

HERA missed the electron-ion phase.  
No deuterons either.  
cf HERA3 in 2001..

Note that **LHeC may be tuned to low energies**  
 $v_s \approx 100$  GeV instead of 1 TeV – direct overlap  
EICs and HERA.

**FCC-eh: highest  $Q^2$ ,  $1/x$**

Expect saturation of rise at  
 $Q_s^2 \approx xg \alpha_s \approx c x^{-\lambda} A^{1/3}$   
Note that the gluon is valence like at low  $Q^2$



**Luminosity:** crucial for efficient operation, to access rare channels and high  $x$ , and  $Q^2$   
15 years of HERA luminosity collection may shrink to a few days (ATLAS now up to  $1\text{fb}^{-1}/\text{day}$ )